

Article

Optimal Planning of Battery Swapping Stations Incorporating Dynamic Network Reconfiguration Considering Technical Aspects of the Power Grid

Waleed Khalid Mahmood Al-Zaidi *  and Aslan Inan 

Electrical Engineering Department, Yildiz Technical University, Istanbul 34220, Turkey; inan@yildiz.edu.tr

* Correspondence: waleed.zaidi@std.yildiz.edu.tr; Tel.: +90-5394782795 or +964-7735950207

Abstract: In order to drive electric vehicle adoption and bolster grid stability, the incorporation of battery swapping stations (BSSs) into the power grid is imperative. Conversely, network reconfiguration plays a crucial role in optimizing energy exchange within the power network, ensuring its economical and safe operation. Therefore, this study proposes an optimal planning method for battery swapping stations that integrates dynamic power distribution network reconfiguration while addressing technical aspects of the grid. The proposed method aims to concurrently optimize the placement and capacity of battery swapping stations, along with power distribution network reconfiguration, to enhance grid reliability and efficiency. The optimization model accounts for various factors including power quality, technical considerations, grid limitations, and operational expenses. A multi-objective optimization framework is devised to simultaneously reduce system losses, improve voltage stability, and mitigate environmental impacts of the power distribution network incorporating DG units. Case studies are conducted to illustrate the efficacy of the proposed approach in enhancing overall grid performance while accommodating the integration of battery swapping stations. The findings underscore the significance of considering technical factors and grid reconfiguration in battery swapping station planning to achieve optimal system operation and maximize benefits for electric vehicle users and grid operators alike.

Keywords: battery swapping stations (BSSs); optimal placement; network reconfiguration; technical and economical criteria



Citation: Al-Zaidi, W.K.M.; Inan, A. Optimal Planning of Battery Swapping Stations Incorporating Dynamic Network Reconfiguration Considering Technical Aspects of the Power Grid. *Appl. Sci.* **2024**, *14*, 3795. <https://doi.org/10.3390/app14093795>

Academic Editor: Manuela Sechilariu

Received: 9 April 2024
Revised: 25 April 2024
Accepted: 26 April 2024
Published: 29 April 2024



Copyright: © 2024 by the authors. Licensee MDPI, Basel, Switzerland. This article is an open access article distributed under the terms and conditions of the Creative Commons Attribution (CC BY) license (<https://creativecommons.org/licenses/by/4.0/>).

1. Introduction

1.1. Research Motivation

Battery swapping stations provide a convenient and effective solution for addressing concerns about electric vehicle (EV) range anxiety and charging times, thereby expediting the shift toward sustainable transportation. Nonetheless, the successful incorporation of battery swapping stations into the power grid necessitates meticulous planning and optimization to ensure dependable and economical operation. Furthermore, the importance of power network reconfiguration lies in its capacity to optimize energy distribution, bolster grid reliability, and ensure the efficient functioning of the electrical system. Through dynamic adjustments to the power network configuration, it becomes feasible to adapt to fluctuations in demand, mitigate voltage variations, and minimize transmission losses. Additionally, network reconfiguration assumes a critical role in the assimilation of renewable energy sources, accommodating the growing presence of distributed generation and facilitating the adoption of emerging technologies like electric vehicles and battery storage systems. Consequently, the synchronized deployment of battery swapping stations coupled with power network reconfiguration can aid in mitigating peak demand, reducing system losses, enhancing voltage stability, and supporting the integration of renewable energy sources, aspects that have been overlooked in recent research efforts.

1.2. Research Literature Review

The incorporation of battery swapping stations into the power grid presents a promising solution to tackle the challenges associated with EV charging infrastructure. However, ensuring the optimal planning of these stations is paramount, particularly when considering dynamic power distribution network reconfiguration and technical intricacies of the power grid, to ensure their efficient operation. This review critically assesses the recent literature pertaining to the optimal planning of battery swapping stations, with a specific emphasis on their integration with dynamic power distribution network reconfiguration and the technical considerations inherent in the power grid. This review scrutinizes various methodologies, identifies challenges, explores opportunities, and delineates potential future research directions in this rapidly evolving domain. Reference [1] focuses on determining the ideal size and location of battery swapping stations while accounting for power system reliability and fluctuations in load. While it underscores the necessity for robust infrastructure planning to guarantee the dependable operation of battery swapping stations within the power grid, it may fall short in fully incorporating dynamic power distribution network reconfiguration or offering comprehensive insights into technical grid aspects, potentially undermining the robustness of the planning approach. Reference [2] delves into the optimal allocation of battery swapping stations, with a keen eye on system reliability. It underscores the importance of strategically siting these stations to bolster the overall reliability of the power distribution network. Nevertheless, it may lack a comprehensive integration of dynamic power distribution network reconfiguration or a thorough consideration of technical grid aspects, potentially leading to less effective planning outcomes. Reference [3] employs particle swarm optimization (PSO) to ascertain the optimal placement and size of battery swapping stations. By leveraging advanced optimization techniques, the study endeavors to enhance the efficiency and efficacy of battery swapping station planning. However, it may not fully integrate dynamic power distribution network reconfiguration or comprehensively address technical grid aspects, potentially diminishing the planning approach's effectiveness. Reference [4] places significant emphasis on user convenience as a pivotal factor in determining the optimal placement of battery swapping stations. The research endeavors to augment the accessibility and usability of battery swapping infrastructure to encourage the widespread adoption of electric vehicles. Despite its focus on user-centric considerations, it may lack a holistic integration of dynamic power distribution network reconfiguration or a comprehensive examination of technical grid aspects, potentially compromising the planning process. Reference [5] investigates the optimal sizing of battery swapping stations, taking into account the dynamic loading patterns of electric vehicles. By analyzing the varying demand for charging, the study aims to optimize the capacity of battery swapping stations to efficiently meet fluctuating demand. However, it may not thoroughly integrate dynamic power distribution network reconfiguration or comprehensively address technical grid aspects, potentially resulting in suboptimal sizing decisions for battery swapping stations. Reference [6] addresses the challenges posed by uncertain loads in the optimal siting and sizing of battery swapping stations. The research explores methodologies to mitigate the impact of load variability on the performance and reliability of battery swapping infrastructure. However, it may not fully incorporate dynamic power distribution network reconfiguration or comprehensively address technical grid aspects, potentially limiting the robustness of the planning decisions. Reference [7] considers demand response mechanisms in determining the optimal placement and size of battery swapping stations. By incorporating demand-side management strategies, the study aims to optimize the utilization of battery swapping infrastructure while bolstering grid stability. Nonetheless, it may lack a comprehensive integration of dynamic power distribution network reconfiguration or a thorough examination of technical grid aspects, potentially compromising the planning approach. Reference [8] delves into the optimal siting and sizing of battery swapping stations while considering the uncertainty associated with renewable energy sources and electric vehicle loads. The research endeavors to enhance the resilience of battery swapping infrastructure amidst variable inputs

and demand. However, it may not fully integrate dynamic power distribution network reconfiguration or offer comprehensive insights into technical grid aspects, potentially diminishing the planning approach's robustness. Reference [9] focuses on the optimal allocation of battery swapping stations, accounting for load uncertainty. By considering variations in demand, the study aims to optimize the distribution of battery swapping infrastructure to maximize grid reliability and efficiency. However, it may not comprehensively integrate dynamic power distribution network reconfiguration or thoroughly address technical grid aspects, potentially leading to less effective planning outcomes. Reference [10] investigates the optimal sizing and location of battery swapping stations in distribution networks witnessing increasing electric vehicle penetration. The research aims to support the seamless integration of electric vehicles into the grid by strategically siting and sizing battery swapping infrastructure. Nevertheless, it may not fully incorporate dynamic power distribution network reconfiguration or comprehensively address technical grid aspects, potentially leading to less efficient planning decisions. Reference [11] incorporates battery degradation into the determination of the optimal size of battery swapping stations. By factoring in the impact of degradation on battery performance, the study aims to prolong the lifespan of battery swapping infrastructure and minimize operational costs. However, it may not comprehensively integrate dynamic power distribution network reconfiguration or offer comprehensive insights into technical grid aspects, potentially compromising the sizing decisions. Reference [12] explores the optimal siting and sizing of battery swapping stations while considering constraints imposed by the power grid. The research endeavors to ensure compatibility with existing infrastructure and minimize the impact on grid operations. Nevertheless, it may not fully integrate dynamic power distribution network reconfiguration or comprehensively address technical grid aspects, potentially resulting in less optimal siting and sizing decisions. References [13,14] investigate optimal sizing and siting considering constraints imposed by the power grid. By accounting for grid limitations, these studies aim to optimize the placement and capacity of battery swapping infrastructure to enhance grid reliability and efficiency. However, they may not comprehensively integrate dynamic power distribution network reconfiguration or thoroughly address technical grid aspects, potentially leading to suboptimal planning outcomes. Reference [14] delves into optimal sizing and siting considering multiple sources of uncertainty. By considering various factors such as load variability and renewable energy integration, the research aims to develop robust battery swapping infrastructure resilient to uncertainties. However, it may not fully integrate dynamic power distribution network reconfiguration or offer comprehensive insights into technical grid aspects, potentially compromising the planning approach's effectiveness. Reference [15] addresses optimal placement and sizing considering the integration of renewable generation. By strategically locating and sizing battery swapping stations, the study aims to facilitate the seamless integration of renewable energy sources into the grid. Nonetheless, it may not comprehensively integrate dynamic power distribution network reconfiguration or thoroughly address technical grid aspects, potentially leading to suboptimal planning decisions. Reference [16] investigates optimal planning considering electric vehicle penetration and distribution network loss. By accounting for these factors, the research aims to optimize the placement and capacity of battery swapping infrastructure to minimize losses and enhance efficiency. However, it may not fully integrate dynamic power distribution network reconfiguration or offer comprehensive insights into technical grid aspects, potentially resulting in less effective planning decisions. Reference [17] addresses optimal planning considering load variability and system uncertainty. By incorporating these factors, the study aims to develop robust battery swapping infrastructure capable of adapting to changing conditions and uncertainties. Nevertheless, it may not comprehensively integrate dynamic power distribution network reconfiguration or thoroughly address technical grid aspects, potentially compromising the planning approach's effectiveness. Reference [18] investigates optimal sizing considering electric vehicle charging behavior. By analyzing charging patterns and behaviors, the research aims to optimize the capacity of battery swapping

stations to effectively meet demand. However, it may not fully integrate dynamic power distribution network reconfiguration or offer comprehensive insights into technical grid aspects, potentially leading to suboptimal sizing decisions. Reference [19] addresses optimal sizing and allocation considering load uncertainty. By accounting for variations in demand, the study aims to optimize the distribution of battery swapping infrastructure to improve grid reliability and resilience. However, it may not comprehensively integrate dynamic power distribution network reconfiguration or thoroughly address technical grid aspects, potentially leading to less effective allocation decisions. Reference [20] investigates optimal placement and sizing considering renewable energy integration. By integrating renewable energy sources, the research aims to develop sustainable battery swapping infrastructure aligned with decarbonization goals. However, it may not fully integrate dynamic power distribution network reconfiguration or offer comprehensive insights into technical grid aspects, potentially compromising the planning approach's sustainability. Reference [21] addresses optimal placement considering voltage stability. By ensuring voltage stability, the study aims to enhance the reliability and performance of battery swapping infrastructure within the distribution network. Nonetheless, it may not comprehensively integrate dynamic power distribution network reconfiguration or thoroughly address technical grid aspects, potentially leading to less effective placement decisions. Reference [22] investigates optimal placement and sizing considering electric vehicle charging behavior. By analyzing charging patterns, the research aims to optimize the capacity and distribution of battery swapping infrastructure to effectively meet demand. However, it may not fully integrate dynamic power distribution network reconfiguration or offer comprehensive insights into technical grid aspects, potentially leading to suboptimal planning decisions. Reference [23] addresses optimal sizing and siting with high penetration of electric vehicles. By considering the impact of electric vehicle adoption, the study aims to develop scalable battery swapping infrastructure capable of accommodating increasing demand. Nevertheless, it may not comprehensively integrate dynamic power distribution network reconfiguration or thoroughly address technical grid aspects, potentially leading to less effective sizing and siting decisions. Upon evaluating the recent state-of-the-art studies, it can be observed that there is a potential lack of comprehensive consideration of dynamic power distribution network reconfiguration or other technical aspects crucial for optimal planning, potentially resulting in suboptimal solutions as evident from these references.

1.3. Shortcomings of Previous Research

Generally, while the references provided offer valuable insights into the optimal planning of battery swapping stations, the following acknowledges the potential shortcomings or limitations that can be expressed about these research studies:

1. **Limited scope:** Some studies may have a narrow focus, addressing specific aspects of optimal planning such as sizing, siting, or allocation, without considering the broader context of dynamic power distribution network reconfiguration or comprehensive technical aspects of the power grid like recent modern research that was performed in [4,5,10,21].
2. **Simplifying assumptions:** Many studies rely on simplifying assumptions or models, which may not fully capture the complexity of real-world scenarios. For example, assumptions about user behavior, load variability, or renewable energy integration could oversimplify the planning process [2,6,21].
3. **Lack of real-world validation:** Some research may lack validation through real-world data or case studies, limiting the applicability and reliability of the proposed methodologies in practical settings [22,24].
4. **Limited consideration of interactions:** The interactions between battery swapping stations and other grid components, such as renewable energy sources, conventional generation, and grid infrastructure, may not be adequately addressed in some studies, leading to suboptimal planning decisions [1,4,19].

5. Neglecting operational challenges: While optimal planning is crucial, operational challenges such as maintenance, grid congestion, cybersecurity, and regulatory constraints are equally important but may receive less attention in the literature [12,15].
6. Limited consideration of stakeholder perspectives: The perspectives and preferences of stakeholders such as utilities, EV owners, policy makers, and local communities may not be adequately incorporated into the planning process, potentially leading to suboptimal solutions [24].
7. Single-objective optimization: Some studies may focus solely on optimizing a single objective, such as cost minimization or grid reliability, without considering trade-offs or multiple conflicting objectives in the planning process [1,3,22].

Addressing these shortcomings could enhance the robustness, applicability, and effectiveness of research on the optimal planning of battery swapping stations in dynamic power distribution networks.

1.4. Research Contribution

In the previous section, the shortcomings of recent state-of-the-art research were assessed. In this section, the following contributions will be presented with the aim of addressing these shortcomings:

1. Technical and economic integration: This paper effectively combines technical aspects of the power grid, such as voltage stability, system losses, grid reliability, sustainability, and integration challenges, with economic goals in the planning process of battery swapping stations. This study aims to ensure efficient and reliable operation within the broader power grid infrastructure.
2. Dynamic network reconfiguration: The importance of dynamically reconfiguring power distribution networks to optimize battery swapping station planning is highlighted. By adjusting network configurations based on real-time demand and supply conditions, the study aims to improve grid flexibility, reliability, and efficiency while accommodating EV integration.
3. Multiobjective optimization: This paper explores techniques for optimizing battery swapping station planning considering multiple objectives such as station capacity, grid constraints, renewable energy integration, and operational scheduling. By adopting a multiobjective approach, this study aims to find optimal solutions that maximize overall system performance.
4. Risk assessment and resilience analysis: Risk assessments and resilience analyses are conducted to identify vulnerabilities, mitigate risks, and improve the ability of battery swapping stations to withstand disruptions. Addressing these aspects contributes to long-term reliability and operational continuity in the face of uncertainties.
5. Environmental impact assessment: Environmental impact assessments are carried out to evaluate the sustainability of battery swapping stations and their potential for reducing carbon emissions in transportation. By assessing the environmental footprint, this study aims to support environmentally friendly infrastructure development and sustainable transportation practices.

In summary, this paper takes a holistic approach to optimizing battery swapping station planning by integrating dynamic network reconfiguration and considering technical aspects of the power grid. Through comprehensive analysis and synthesis of the relevant literature, this study aims to offer insights and recommendations for developing efficient, reliable, and sustainable infrastructure solutions for EV integration within the power grid.

1.5. Structure of the Research

This paper's structure unfolds as follows: Starting with an Introduction section offering an overview, subsequent sections delve into specific aspects. Section 2 elaborates on the conceptual model, followed by Section 3, which outlines the mathematical formulation of the proposed technique. Additionally, Section 4 discusses the incorporation of the proposed approach into a multiobjective optimization framework, demonstrated through a flowchart.

Moving forward, Section 5 focuses on simulating and discussing the results derived from conducted simulations. Concluding the paper, the primary findings of this article are summarized in the Section 6.

2. Problem Statement and Solution Procedure

This section delves into crafting and defining the framework of a novel approach aimed at optimal and safe energy management planning within the context of the BSS placement problem, considering the dynamic reconfiguration of power microgrids. The conceptual model outlining this proposed structure is visually depicted in Figure 1. As illustrated, the opening and closing of dynamic switches trigger shifts in the power network’s topology, consequently altering the flow of energy along power transmission lines. This dynamic process not only affects technical parameters and power quality within the network but also influences economic objectives. Hence, it becomes imperative within the proposed objective function framework to simultaneously factor in the optimal placement of battery swapping stations and the status of dynamic network switches when formulating the objective function. Consequently, further elucidation is provided on the mathematical formulation of the objective function as outlined in the conceptual model.

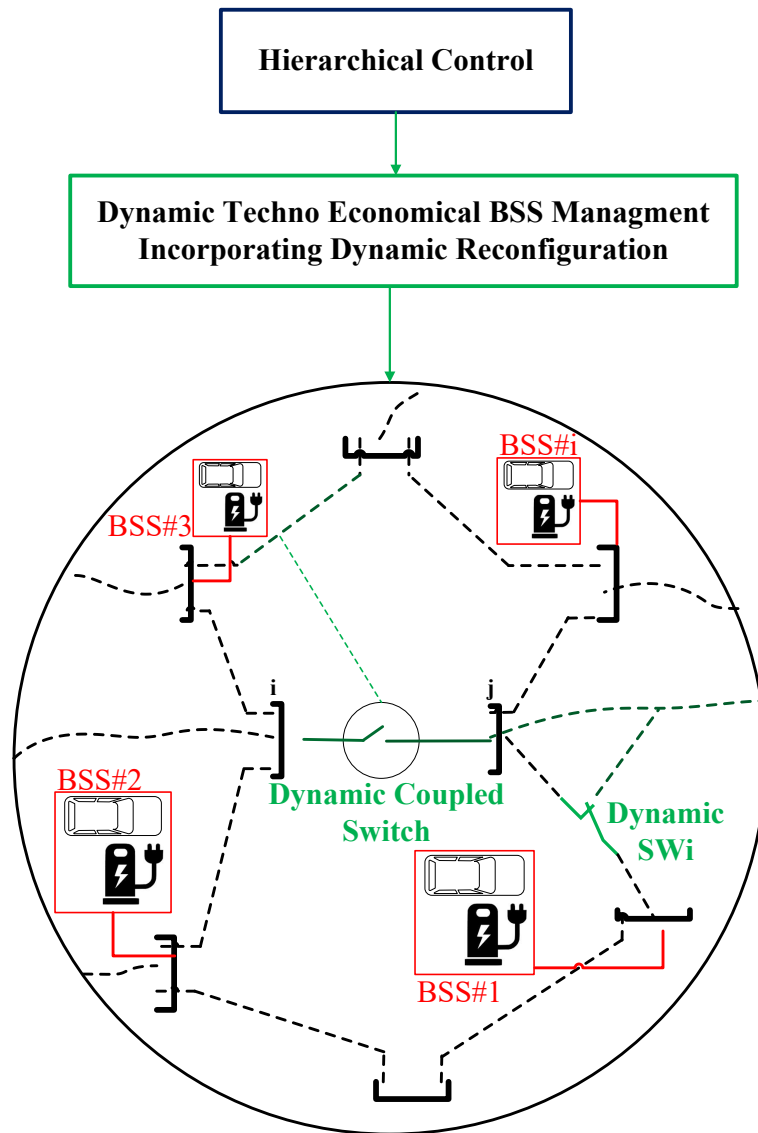


Figure 1. Conceptual model of proposed optimal planning of BSS incorporating dynamic reconfiguration.

3. Mathematical Modeling Formulation

3.1. Modeling of Battery Swapping Station

As previously noted, battery swapping stations function as convenient hubs for integrating electric vehicles into the distribution network, serving as both energy recipients from and contributors to the grid. Hence, the charging status of these vehicles significantly influences the metrics and parameters of the distribution network. This section introduces a robust model tailored for planning and siting analyses aimed at determining the charging status of these vehicles. In this proposed approach, each electric vehicle, whether charging or discharging, is depicted as a voltage source converter (VSC) in accordance with Figures 2 and 3. Consequently, the power received by an electric vehicle from the grid during charging is derived from Equation (1) [24]. This model not only aids in understanding the energy flow dynamics but also facilitates efficient resource allocation and infrastructure planning within the distribution network.

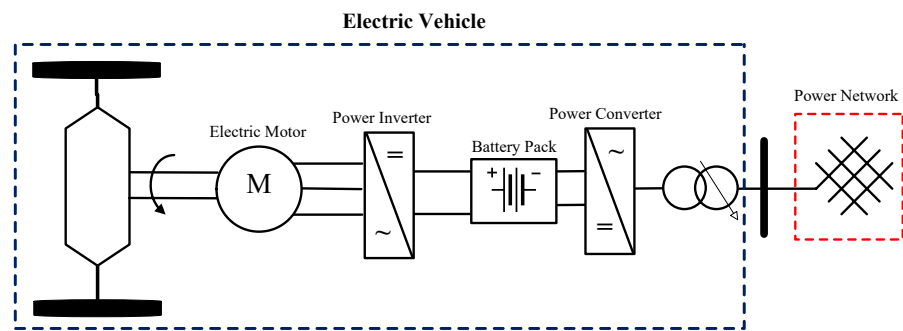


Figure 2. Diagram illustrating the connection between a grid and an electric vehicle charging station.

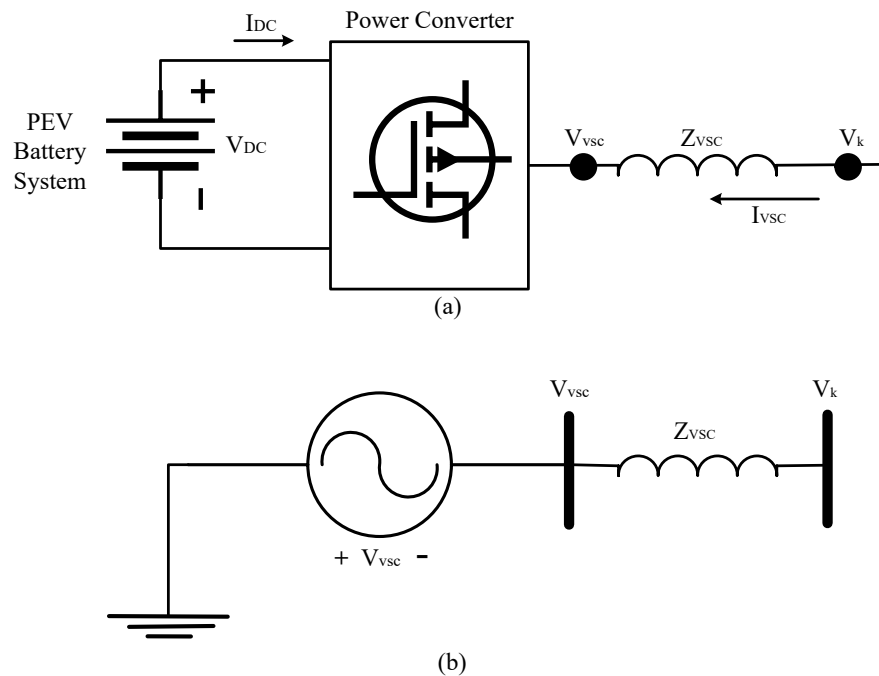


Figure 3. Equivalent representation of an electric vehicle's circuitry when connected to the power grid (a) general configuration, (b) electrical equivalent circuit.

$$P_{EV}^{ch/dis}(t) = P_{EV_{max}}(1 - e^{-\alpha t/t_{max}}) + P_{EV0} \tag{1}$$

where in Equation (1) the following are used:

P_{EV0} represents the initial charging power of the electric vehicle.

α denotes the charging battery time constant of the electric vehicle.

t_{max} signifies the total time needed to charge the electric vehicle’s battery from zero charge to maximum charge.

$P_{EV_{max}}$ stands for the maximum charging power of the electric vehicle.

As illustrated in Figure 4, electric vehicles, whether charging or discharging at charging stations, are electrically interconnected to the grid in both series and parallel configurations. Consequently, the aggregate power consumption or generation by electric vehicle charging stations can be determined utilizing Equation (2) [24].

$$P_{EV}^{total} = \sum_{i=1}^n \sum_{j=1}^m P_{EV,ij} \tag{2}$$

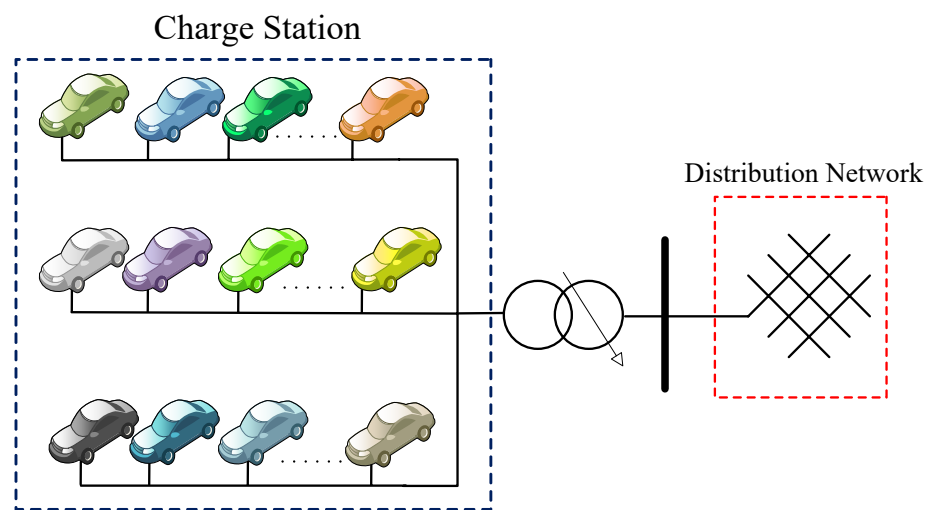


Figure 4. Integration of electric vehicles with a charging station network.

Given that the presence or absence of electric vehicles at charging stations hinges on the probabilistic tendencies of electric vehicle owners and the duration required for discharging or charging, the active power received from the grid by BSS is inherently subject to random and probabilistic behavior. This aspect necessitates careful consideration in the modeling of Equation (2). To address this, BSSs are classified into three categories based on charging speed: slow-charging, medium-charging (battery-switching), and fast-charging stations. In this study, the fast-charging method is employed to model the behavior of fast-charging stations using a probabilistic Markov model. The schematic of the probabilistic Markov model for a fast-charging electric vehicle station is depicted in Figure 5 [25].

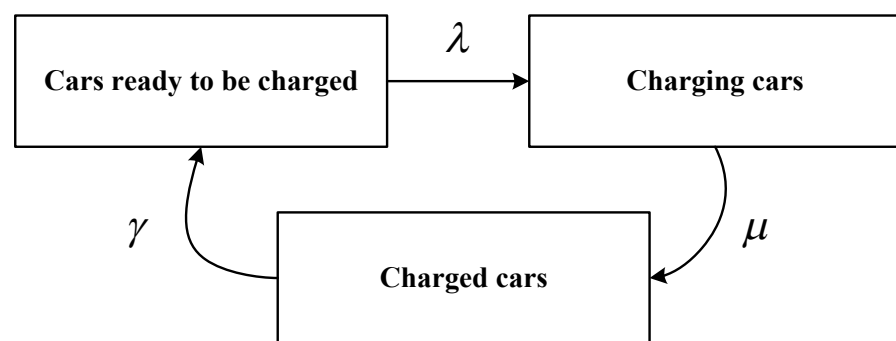


Figure 5. Markov probabilistic model representation for a fast-charging electric vehicle station.

In the provided figure, λ denotes the success rate of a vehicle in accessing the charging converter, μ represents the success rate of a vehicle in completing its battery charging, and γ signifies the rate at which a battery charging for an electric vehicle is completed and transitions to the ready-to-charge state. Hence, referring to Figure 5, the probability coefficient of power consumption in an electric vehicle charging station can be derived as follows from Equations (3) and (4) [25]:

$$P_N = \frac{\left(\frac{c\rho}{N}\right)^N}{N!} \bigg/ \left(\sum_{i=0}^c \frac{1}{i!} \left(\frac{\lambda}{\mu}\right)^i + \sum_{j=c+1}^N \frac{1}{c^{j-c} \cdot c!} \left(\frac{\lambda}{\mu}\right)^j \right) \quad : N < c \quad (3)$$

$$P_N = \frac{\left(\frac{c\rho}{c}\right)^c \cdot (N - c)}{c!} \bigg/ \left(\sum_{i=0}^c \frac{1}{i!} \left(\frac{\lambda}{\mu}\right)^i + \sum_{j=c+1}^N \frac{1}{c^{j-c}} \cdot \frac{1}{c!} \cdot \left(\frac{\lambda}{\mu}\right)^j \right) \quad : N < c \quad (4)$$

In Equations (3) and (4), the following are used:

P_N represents the probability coefficient of power consumption in an electric vehicle charging station.

λ denotes the success rate of a vehicle in accessing the charging converter.

μ signifies the success rate of a vehicle in completing its battery charging.

$\rho = \lambda / \mu \cdot c$ stands for the number of charging stations for electric vehicles.

C represents the number of BSSs for electric vehicles.

Hence, utilizing Equations (2) through (4), the potential power consumption of a charging station can be reformulated as Equation (5):

$$P_{EV,N}^{total} = P_{EV}^{total} \times P_N \quad (5)$$

On the other hand, the operational characteristics dictating the functionality of a BSS are subject to numerous factors. These factors encompass the configuration of battery units, the duration of backup power, temperature conditions, battery longevity, depth of discharge, stipulated power reserves, and the extent of renewable energy integration into the grid, among other variables. Therefore, it becomes imperative to intricately model the charging and discharging processes of vehicle batteries within charging stations, a detailed representation of which is provided in reference [26] as follows:

$$P_{BSS}(t) = P_{ch}(t) \quad : \text{if } \left\{ \sum P_G(t) - P_D(t) \right\} \geq 0. \quad (6)$$

$$P_{BSS}(t) = P_{dis}(t) \quad : \text{if } \left\{ \sum P_G(t) - P_D(t) \right\} < 0. \quad (7)$$

where $P_{BSS}(t)$, $\sum P_G(t)$, and $P_D(t)$ are the powers of BSS, total generation of the system, and load demand, respectively. Furthermore, $P_{ch}(t)$ and $P_{dis}(t)$ are charging and discharging powers of BSS.

Essentially, a BSS unit can function in only one mode at a time, either charging or discharging. The computation for the power of the BSS during the charging phase is outlined as follows:

$$E_{ch}(t) = \left(\frac{\sum P_G(t) - P_D(t)}{\eta_{Conv}} \right) \times \Delta t \times \eta_{ch}. \quad (8)$$

$$SOC(t) = SOC(t - 1)(1 - \sigma) + E_{ch}(t). \quad (9)$$

For the discharging state,

$$E_{dis}(t) = \left(-\frac{\sum P_G(t) - P_D(t)}{\eta_{Conv}} \right) \times \Delta t \times \eta_{dis}. \quad (10)$$

$$SOC(t) = SOC(t - 1)(1 - \sigma) - E_{ch}(t). \quad (11)$$

where in the above equations $SOC(t)$, $E_{ch}(t)$, $E_{dis}(t)$, σ , η_{ch} , η_{dis} , and η_{Conv} represent the battery's charge state, the amount of energy being charged, the amount of energy being

discharged, the rate at which energy is self-discharged, the efficiency of charging and discharging processes, and the efficiency of the converter, respectively. The constraints outlined in Equations (12) and (13) are designed to regulate the energy level and the power involved in charging and discharging operations within the PSS. Furthermore, Equation (14) is implemented to ensure the consistency of the PSS’s energy level throughout the scheduling horizon, guaranteeing that it remains unchanged from the beginning to the end of the specified timeframe.

$$E_{BSS}^{\min(BSS^{\min}, BSS^{\max})} \tag{12}$$

$$P_{BSS}^{\min(BSS^{\min}, BSS^{\max})} \tag{13}$$

$$E_{BSS}^{\text{initial}}(t) = P_{BSS}^{\text{final}}(t) \tag{14}$$

The operating cost of the PSS (C_{bw}) units can be described as

$$C_{BSS} = N_{\text{batt}} \frac{C_{\text{rep, batt}}}{\sqrt{\eta_{rt}}} + C_{BSS}^{\text{constant}} \tag{15}$$

where in Equation (15), $C_{\text{rep, batt}}$, η_{rt} , and $C_{BSS}^{\text{constant}}$ represent the following parameters: the storage replacement cost, the round-trip efficiency of the storage, and the constant cost of the BSS, respectively.

3.2. Modeling of PV and Wind Turbine Power

The generation of renewable energy from sources like solar photovoltaic systems and wind turbines is greatly influenced by the availability of key energy sources such as sunlight and wind. The electricity generated by solar panels is directly linked to the amount of sunlight that reaches the Earth’s surface, a factor that can be influenced by variables like geographical location, weather patterns, and the duration of daylight. Consequently, the efficiency of solar arrays is affected by factors such as cell temperature and the intensity of solar radiation at peak power generation. Equations (16) and (17) [26] can be employed to compute these parameters accurately.

$$P_{PV}(t) = \left[P_{(PV,STC)} \cdot \frac{G_T(t)}{1000} \cdot (1 - \gamma(T_j - 25)) \right] \cdot N_{PVs} \cdot N_{PVp} \tag{16}$$

$$T_j = T_{\text{amp}} + \frac{G_T}{G_{T,STC}} \cdot (NOCT - 20) \tag{17}$$

Equations (16) and (17) define various parameters within the realm of photovoltaic systems. Specifically, the symbols represent the following attributes: P_{PV} denotes the output power of the photovoltaic system at maximum power point, and $P_{PV,STC}$ denotes the rated power of the photovoltaic system; G_T represents the radiation level under standard conditions; γ signifies the temperature coefficient of power at the maximum power point; T_j stands for the temperature of solar cells; N_{PVs} , N_{PVp} signify the number of modules arranged in series and parallel, respectively; and finally, $NOCT$ denotes the nominal operating temperature of the cell. Furthermore, the power output from wind turbines P_{wt} is intricately linked to the velocity of the wind, a factor subject to fluctuations across different timeframes, ranging from instantaneous changes to hourly, daily, and seasonal variations. Hence, Equation (18) is utilized to model the actual power generation of a wind turbine [26].

$$P_{wt}(v) = \begin{cases} 0 & \text{if } v < V_{ci} \\ P_R(A + Bv + Cv^2) & \text{if } V_{ci} < v < V_r \\ P_R & \text{if } V_r < v < V_{co} \\ 0 & \text{if } V_{co} < v \end{cases} \tag{18}$$

In Equation (18), P_{wt} , V_{ci} , V_{co} , and V_r represent the wind turbine output power, cut-in, cut-out, and rated wind speeds, respectively. The variable A denotes the rated power of the wind turbine, while B and C symbolize the coefficients linked with the turbine.

3.3. Cost Formulation of Renewable and Traditional Generation Units

In general, the cost function of wind and photovoltaic units is defined as a first-degree function according to Equation (19) [26].

$$\text{Cost}_{(RE)} = \begin{cases} \zeta_R P_R + \psi_R^{cte} & : \text{if } 0 < P_R < P_R^{\max} \\ 0 & : \text{if } P_R = 0 \end{cases} \quad (19)$$

In this equation, ζ_R represents the variable cost associated with renewable generation units, P_R denotes the output power of these renewable units, and ψ_R^{cte} signifies the constant costs related to the renewable units. On the other hand, Equation (20) characterizes the generation cost of the traditional distributed generation units such as microturbines and diesel generators. It encapsulates both operational expenses in the form of a second-order equation and the costs attributed to environmental pollution as a first-order Equation [26].

$$\text{Cost}_{(TR)} = \begin{cases} \underbrace{(\kappa_T P_T^2 + \zeta_T P_T + \gamma_T)}_{\text{Operational Cost}} + \underbrace{((\lambda_{CO_2} \times CO_2 + \lambda_{SO_2} \times SO_2 + \lambda_{NO_x} \times NO_x))}_{\text{Pollution Cost}} & : \text{if } 0 < P_T < P_T^{\max} \\ 0 & : \text{if } P_T = 0 \end{cases} \quad (20)$$

The parameters specified in Equation (20) are outlined as follows:

$\lambda_{(CO_2)}$ represents the penalty factor associated with CO_2 emissions.

$\lambda_{(SO_2)}$ signifies the penalty factor related to SO_2 emissions.

$\lambda_{(NO_x)}$ indicates the penalty factor linked to NO_x emissions.

Ultimately, the overall cost function of generation units can be expressed in the following manner:

$$\text{Obj}_1 = \text{Total Cost} = \text{Cost}_{TR} + \text{Cost}_{RE} \quad (21)$$

3.4. Mathematical Formulation of Technical Objectives

3.4.1. Power Losses and Loss Sensitivity Index

Minimizing power network losses is a crucial goal for microgrid planners and operators of smart distribution networks because these losses can restrict transmission capacity and lead to increased operational expenses. Therefore, the total losses within distribution networks play a significant role in the optimization process, as reflected in the computation outlined in Equation (22). By prioritizing the reduction of these losses, stakeholders can enhance the efficiency and reliability of their systems while also potentially reducing operational costs and environmental impacts [26].

$$\text{Obj}_2 = \text{Losses} = \underbrace{\left(|V|^2 / R_{Z_i} \right)_{\text{end}} - \left(|V|^2 / R_{Z_i} \right)_{\text{start}}}_{\text{Active Losses}} + \underbrace{\left(|V|^2 / X_{Z_i} \right)_{\text{end}} - \left(|V|^2 / X_{Z_i} \right)_{\text{start}}}_{\text{Reactive Losses}} \quad (22)$$

On the other hand, the power loss sensitivity factor (PLSF) serves as a valuable tool for assessing the susceptibility of individual buses within the network to changes in active power injection and their impact on overall power losses, as detailed in Equation (23). This metric is utilized to pinpoint the most favorable bus locations for integrating distributed generation (DG) within a radial distribution system (RDS). By analyzing the PLSF values of each bus in the network, planners can identify strategic sites with high sensitivity, indicating

their suitability for DG deployment. This approach allows for targeted placement of DG resources to optimize system performance and enhance overall network efficiency.

$$Obj_3 = PLSF = \sum_{i=1}^N \left(\frac{\partial P_{loss(i,i+1)}}{\partial P(i+1)} \right) = \sum_{i=1}^N R_i \left(\frac{2P(i+1)}{|V(i+1)|^2} \right) \quad (23)$$

3.4.2. Voltage Deviation Index

The aim of this research is to minimize voltage variations in the distribution grid during the integration of BSSs. The extent of voltage fluctuation can be quantified by employing the formula provided in Equation (24) [26]. This study focuses on developing strategies to mitigate voltage deviations effectively, thereby enhancing the stability and reliability of the distribution network when incorporating BSS technology.

$$Obj_4 = VD = \sqrt{\sum_{i=1}^N \left(\frac{V_{Standard}}{V_{Base}} - \frac{V_i}{V_{Base}} \right)^2} \quad (24)$$

3.4.3. Short-Circuit Level Index

The short-circuit level plays a pivotal role in the network’s technical dynamics, being significantly influenced by variations in generation, consumption, and network configuration. This critical parameter directly impacts protection settings and network planning, thereby influencing the overall safety and efficiency of the network. When strategically deploying BSSs, it is imperative to take into account this often overlooked factor. Failure to consider the short-circuit level can lead to potential damages due to inadequate protection system performance during BSS charge–discharge cycles and diverse generation sources. Therefore, a comprehensive energy management strategy must incorporate defining and addressing the short-circuit level to ensure network stability amidst fluctuations in generation capacity and network layout. This research paper aims to provide a clear definition of the short-circuit level within the context of energy management strategies [26].

$$Obj_5 = SCLI = \left(\sum_{k=1}^{nb} \left(1 - \frac{(V_k^*)}{(Z_{kk} + Z_f)} \bigg/ \frac{V_k}{(Z_{kk} + Z_f)} \right) \right) \quad (25)$$

In the equations provided above, V_k and V_k^* denote the voltage at a bus in the network before and after any modifications to the network. Z_{kk} and Z_f refer to the impedance of the bus itself and the impedance of the fault that occurred at that particular bus in the network, respectively.

3.4.4. Voltage Sensitivity Index

The Voltage sensitivity index (VSI) holds significant importance in power distribution networks and microgrids, serving as a crucial indicator of system security and power quality. It assesses the network’s capability to uphold stable voltage levels amidst escalating consumer demand, thereby reflecting the system’s overall safety. This research endeavors to enhance network security by elevating the VSI to a pivotal objective. The concept of VSI is designed to illustrate a decline as the system load intensifies, ultimately converging towards zero as the network approaches a critical state of collapse and reaches its maximum sustainable load capacity. This study aims to refine the understanding and application of the VSI within energy management strategies to fortify network resilience and reliability under varying operational conditions [26].

$$Obj_6 = VSI = \sum_{i=1}^N \left(|V_i|^4 - 4|V_i|^2 \left(R_{eq,i} P_{Lm,i} + X_{eq,i} Q_{Lm,i} \right) - 4 \left(X_{eq,i} P_{Lm,i} - R_{eq,i} Q_{Lm,i} \right)^2 \right) \quad (26)$$

In Equation (26), the variable $|V_i|$ represents the voltage magnitude at bus i , whereas $R_{eq,i}$ and $X_{eq,i}$ stand for the total resistance and reactance of the line. Furthermore, the symbols $P_{LM,i}$ and $Q_{LM,i}$ correspond to the aggregate active and reactive power of all nodes, respectively. This equation encapsulates the interplay between voltage levels, line characteristics, and power flow distribution within the network, highlighting the intricate relationship between these key parameters in ensuring efficient and stable operation.

3.4.5. Expected Energy Not Served (EENS) Index

In the domain of power distribution networks and microgrids, evaluating network reliability is a critical focal point in planning and operational analyses. Various metrics are examined to measure network reliability, with the expected energy not served (EENS) index emerging as a particularly practical and versatile indicator for assessing reliability across different energy generation and transmission levels. This index, also utilized in the referenced paper [27], plays a crucial role in comprehensively evaluating the reliability of power systems, underscoring its significance in ensuring efficient and robust network operations:

$$Obj_7 = EENS = \underbrace{\left(\sum_{i=1}^{N_G} \rho_i^G E_{(i,P_{G_i}^{Outage})}^G \right)}_{EENS \text{ of } G} + \underbrace{\left(\sum_{j=1}^{N_L} \rho_j^L E_{(i,L_i^{Outage})}^L \right)}_{EENS \text{ of } L} \quad (27)$$

3.5. Modeling of Switching in Dynamic Reconfiguration

Figure 6 illustrates the intricate interconnections between the components of a distribution network and microgrids via power distribution lines. The dynamic reconfiguration of this network and its linked microgrids is facilitated by the controlled operation of circuit breakers within the system. This enables the adjustment of power network configurations by manipulating the opening and closing of switches during network operations, facilitating energy exchange between different segments of the network. Consequently, the coupling switches in the network play a pivotal role in altering the power distribution pathways through their opening and closing actions. To represent the states of these switches within the network, a binary formulation is utilized, where a value of 0 signifies the open state and 1 indicates the closed state, as detailed in Equation (28).

$$S_i = \begin{cases} 1 & \text{if Switch is closed} \\ 0 & \text{if Switch is opened} \end{cases} \quad (28)$$

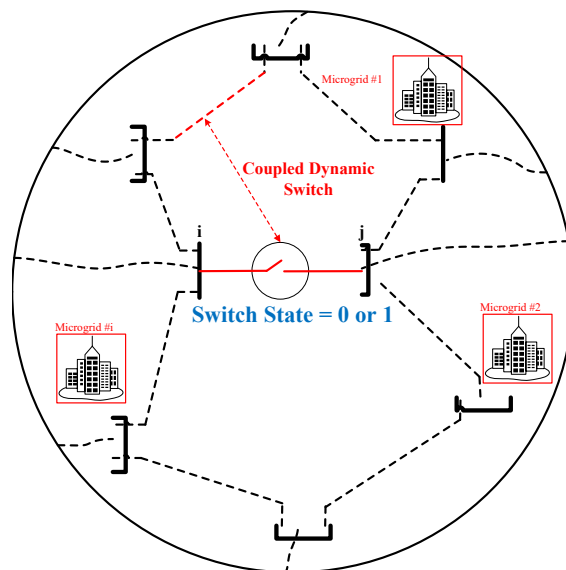


Figure 6. Various forms of dynamic switching within the proposed framework.

3.6. Formulation of the Objective Function

The optimization model proposed in this study is tailored to tackle a complex challenge with multiple competing goals. In contrast to conventional optimization problems, it does not have a singular solution, but rather, any feasible solution that meets the specified constraints can be deemed optimal. The primary objective is to balance safety and efficiency in the deployment of BSSs and the dynamic configuration of switches, considering factors such as unit commitment, controllable distributed generation capacities, and power interactions with the main network for each hour ahead. The overarching goal of this comprehensive planning is to ensure both optimal and secure operations by considering all technical network parameters while accommodating the charging and discharging activities of BSSs and dynamic switches over time. To achieve this, a novel multiobjective optimization strategy is devised based on the gray wolf optimization technique. The planning challenge is framed as a multiobjective function, as depicted in Equation (29), aiming to strike a balance between conflicting objectives and constraints effectively.

$$\min \text{OBJ}_{\text{total}} = \min \{ \text{Obj}_k(N_{\text{BSS}}, L_{\text{BSS}}, C_{\text{BSS}}, S_{0,1}) \}_{k=1,\dots,7} \quad (29)$$

In the equation provided, the variables N_{BSS} and L_{BSS} denote the quantity and location of battery storage systems (BSSs), while the parameters C_{BSS} and $S_{0,1}$ represent the capacity of the BSSs and the statuses of dynamic switches in the objective functions of the planning problem under consideration. Consequently, the objective functions sought in this research can be articulated as a set of seven interconnected objectives to address the complexities of the planning scenario at hand as follows:

$$\min \text{OBJ}_{\text{total}} = \min \left\{ \begin{matrix} [\gamma_1 \ \gamma_2 \ \dots \ \gamma_k] \\ \begin{bmatrix} \text{Obj}_1(N_{\text{BSS}}, L_{\text{BSS}}, C_{\text{BSS}}, S_{0,1}) \\ \text{Obj}_2(N_{\text{BSS}}, L_{\text{BSS}}, C_{\text{BSS}}, S_{0,1}) \\ \vdots \\ \text{Obj}_k(N_{\text{BSS}}, L_{\text{BSS}}, C_{\text{BSS}}, S_{0,1}) \end{bmatrix} \end{matrix} \right\}_{k=1,\dots,7} \quad (30)$$

In Equation (30), the variable γ_k symbolizes the weight coefficient associated with the objective functions. When adjusting these weights for each objective function, it is crucial to consider specific events and system characteristics, such as varying system states during maintenance, replacement schedules, the probability of component failures, and diverse error occurrences within the system, each resulting in unique system performance conditions. These weights are fine-tuned to accurately reflect the importance of these events and characteristics within the overarching optimization framework. By assigning higher weights to certain objective functions, their impact on the optimization process is amplified, indicating their relative significance in achieving the desired system performance levels. The process of adjusting these weights involves a thorough assessment of each event and system attribute to ensure an optimal and well-rounded solution for the multiobjective optimization task.

4. Enhanced Multiobjective Optimization Method Based on GWO

In essence, multiobjective optimization involves addressing multiple goals at once. In the context of this study, these goals encompass technical, economic, and reliability aspects of the system, as elaborated in the preceding section. Consequently, the optimization problem can be mathematically formulated to either minimize or maximize certain criteria [28].

$$\begin{aligned} \text{Optimize:} \quad & \text{Total OBJ}(\vec{X}) = \{ \text{obj}_1(\vec{x}), \text{obj}_2(\vec{x}), \dots, \text{obj}_n(\vec{x}) \} \\ \text{subject to:} \quad & \psi_i(\vec{x}) \geq 0, \quad i = 1, 2, \dots, \nu \\ & \theta_i(\vec{x}) = 0, \quad i = 1, 2, \dots, \sigma \\ & U_i^{\text{lb}} \leq x_i \leq U_i^{\text{ub}}, \quad i = 1, 2, \dots, \gamma \end{aligned} \quad (31)$$

In the above equation, ν represents the count of inequality constraints, σ denotes the number of equality constraints, γ stands for the number of variables, ψ_i signifies the i th inequality constraint, ρ_i indicates the number of objective functions, ϑ_i denotes the i th equality constraint, and $[U_i^{lb}$ and $U_i^{ub}]$ represent the boundaries of the i th variable. It is evident that traditional relational operators fall short in effectively comparing solutions across multiple objectives. In the current study, the predominant operator utilized is Pareto optimal dominance, which is defined as follows for minimization problems:

$$\forall n \in \{1, 2, \dots, \gamma\} : \text{obj}_n(\vec{x}) \leq \text{obj}_n(\vec{y}) \quad \wedge \quad \exists n \in \{1, 2, \dots, \gamma\} : \text{obj}_n(\vec{x}) < \text{obj}_n(\vec{y}) \tag{32}$$

where in Equation (32), $\vec{x} = (x_1, x_2, \dots, x_\gamma)$ and $\vec{y} = (y_1, y_2, \dots, y_\gamma)$. These equations demonstrate that a solution surpasses another in a multiobjective search space when it matches all objectives and outperforms in at least one objective. The principle of Pareto optimal dominance is symbolized by \prec and \succ , which allow for straightforward comparison and distinction between solutions. In population-based multiobjective algorithms, solutions consist of multiple solutions. However, the exact determination of the optimal solution is challenging due to each solution being constrained by other objectives, leading to inherent conflicts between objectives. Therefore, the primary function of stochastic or population-based multiobjective algorithms is to identify the best trade-offs among objectives, resulting in what is known as a Pareto optimally set. In the gray wolf optimization (GWO) framework, the hierarchy among solutions designates the most optimal as alpha, followed by beta and delta, representing the second- and third-best solutions, respectively. The remaining solutions are collectively termed omega. Within the GWO algorithm, the strategic pursuit is orchestrated by beta and delta, while the gamma solution trails behind these key wolves. When the prey is cornered and ceases to move, the assault on the leadership of the alpha wolf commences. The orchestration of this process is facilitated through the manipulation of the reduction vector ‘a’. This vector, denoted as ‘A’, is subject to randomization within the range $[-2a, 2a]$. By diminishing ‘a’, the coefficients of vector ‘A’ are likewise reduced. Should the magnitude of ‘A’ fall below 1, it signifies the convergence of the alpha wolf (and others) towards the prey, while a magnitude exceeding 1 indicates a movement away from the prey. The gray wolf optimization algorithm necessitates the synchronization of all wolves, compelling them to adjust their positions in accordance with the movements of the alpha, beta, and delta wolves. In the pursuit scenario, gray wolves tactically encircle their prey. This encirclement behavior is mathematically modeled through the following equations, where ‘t’ denotes the current iteration, ‘A’ and ‘C’ stand for coefficient vectors, ‘Xp’ represents the position vector of the prey, and ‘X’ signifies the position vector of the gray wolf:

$$\vec{D} = |\vec{C} \cdot \vec{X}_p(t) - \vec{X}(t)| \tag{33}$$

$$\vec{X}(t + 1) = \vec{X}_p(t) - \vec{A} \cdot \vec{D} \tag{34}$$

Vectors A and C are calculated as follows:

$$\vec{A} = 2\vec{a} \cdot \vec{r}_1 - \vec{a} \tag{35}$$

$$\vec{C} = 2 \cdot \vec{r}_2 \tag{36}$$

In the given equations, the variable ‘a’ undergoes a linear decrease from 2 to 0 over the course of iterations, while ‘r1’ and ‘r2’ represent random vectors falling within the range $[0, 1]$. Typically, the hunting expedition is predominantly orchestrated by the alpha, although the beta and delta wolves may intermittently join in. Within the mathematical framework depicting gray wolf behavior during the hunt, it is assumed that alpha, beta, and delta possess superior knowledge regarding potential prey positions. The positions of the top three solutions are retained, compelling other wolves to adjust their positions

in accordance with those of the highest-ranked agents, as delineated by the provided equations.

$$\begin{aligned} \vec{D}_\alpha &= |\vec{C}_1 \cdot \vec{X}_\alpha - \vec{X}| \\ \vec{D}_\beta &= |\vec{C}_2 \cdot \vec{X}_\beta - \vec{X}| \end{aligned} \tag{37}$$

$$\begin{aligned} \vec{D}_\delta &= |\vec{C}_3 \cdot \vec{X}_\delta - \vec{X}| \\ \vec{X}_1 &= \vec{X}_\alpha - \vec{A}_1 \cdot \vec{D}_\alpha \\ \vec{X}_2 &= \vec{X}_\beta - \vec{A}_2 \cdot \vec{D}_\beta \end{aligned} \tag{38}$$

$$\begin{aligned} \vec{X}_3 &= \vec{X}_\delta - \vec{A}_3 \cdot \vec{D}_\delta \\ \vec{X}(t+1) &= \frac{\vec{X}_1 + \vec{X}_2 + \vec{X}_3}{3} \end{aligned} \tag{39}$$

In this investigation, both the quantitative and qualitative efficacy of the proposed MOGWO algorithm is evaluated. To gauge its performance, a novel formulation for generational distance is employed. This formulation serves to depict the distribution of nondominated solutions acquired through the algorithm. Here is the proposed representation:

$$\Phi = \sqrt{\frac{1}{NPFS - 1} \int_{i=1}^{NPFS} (D_i - D)^2 di} \tag{40}$$

Here, D represents the average of all D_i , where $NPFS$ denotes the total number of achieved Pareto optimal solutions, and D_i is defined as follows:

$$D_i = \min_{1 \leq i, j \leq n} (|obj_1^i(\vec{x}) - obj_1^j(\vec{x})| + |obj_2^i(\vec{x}) - obj_2^j(\vec{x})|) \tag{41}$$

The minimum value of the ϕ metric indicates that the globally optimal nondominated solutions are evenly spread out. Therefore, when the numerical values of D_i and D are identical, the ϕ metric will be zero, signifying a balanced distribution of solutions. The process flowchart for the improved optimization method using the gray wolf optimization (GWO) algorithm is presented in Figure 7.

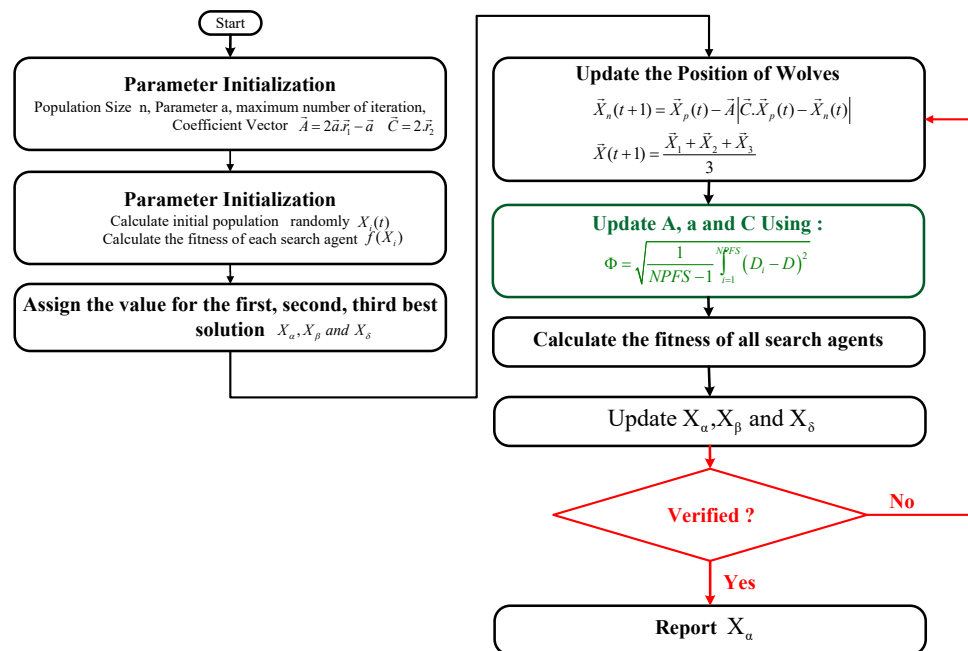


Figure 7. Flowchart illustrating the optimization process of the modified gray wolf algorithm.

5. Result Analysis and Discussion

In this section, this paper explores a proposed method for evaluating the strategic placement of BSSs and dynamic reconfiguration in intelligent distribution networks like the IEEE 118-, 69-, and 33-bus systems and their subnetworks. The assessment considers various load conditions, ranging from 20% to 150% of the rated load, as depicted in Figure 8 for different case studies. To validate this methodology, the authors utilize a 118-bus distribution network with interconnected microgrids, as shown in Figure 9, comparing it with recent approaches in the field. For detailed information on load data and network lines, readers are advised to refer to the provided source [26]. In this study, three microgrids are positioned at nodes 1, 26, and 111. Additionally, specific lines between buses 11–12, 68–69, and 104–105 are coupled with the lines between buses 17–27, 80–99, and 91–115 in the network, respectively. In this regard, Table 1 shows the dynamic coupled switches in each case study. The distributed generation resources in these microgrids include wind turbines, photovoltaic systems, microturbines, and diesel generators to provide operational power. The optimal placement of BSSs is conducted during system operation. The proposed method is then assessed and compared with recent methods, considering network security and reliability indicators. A multiobjective optimization algorithm is employed to optimize the mentioned function, and its results are evaluated against other optimization algorithms discussed.

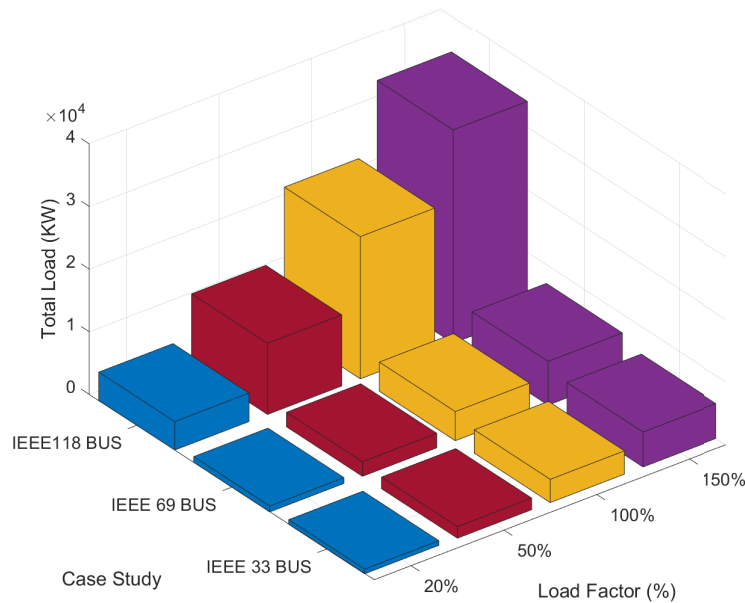


Figure 8. Different load factor scenarios for each case study of IEEE 33, 69, and 118 bus.

Table 1. Initial states of dynamic coupled switches in each case study.

Switch Number	IEEE 118 Bus		IEEE 69 Bus		IEEE 33 Bus	
	Coupled Switch Location		Coupled Switch Location		Coupled Switch Location	
	Normally open	Normally closed	Normally open	Normally closed	Normally open	Normally closed
1	Bus17–Bus27	Bus11–Bus12	Bus46–Bus15	Bus3–Bus36	Bus25–Bus29	Bus3–Bus23
2	Bus80–Bus99	Bus68–Bus69	Bus20–Bus65	Bus9–Bus53	Bus5–Bus33	Bus6–Bus26
3	Bus91–Bus115	Bus104–Bus105	Bus5–Bus35	Bus3–Bus28	Bus12–Bus22	Bus2–Bus19

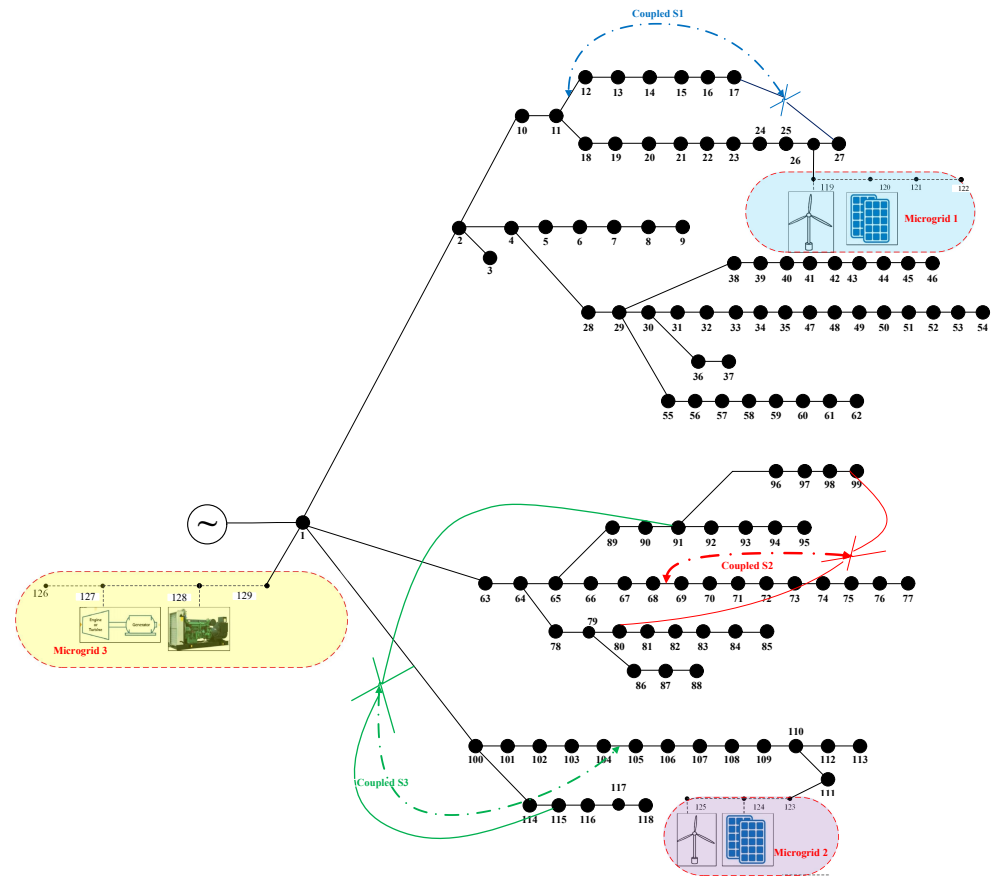


Figure 9. Schematic of IEEE 118-bus case study involving microgrids and dynamic switches.

5.1. Input Data Analysis

As mentioned in the previous section, the advanced distribution network, combined with its interconnected microgrids, utilizes decentralized power sources like wind turbines and photovoltaic systems to produce electricity. Figures 10–12 further depict the patterns of solar radiation, ambient temperature, wind speed, and load consumption at different load factor intervals within the network. These visuals provide a comprehensive overview of the dynamic factors influencing power generation and consumption in the system.

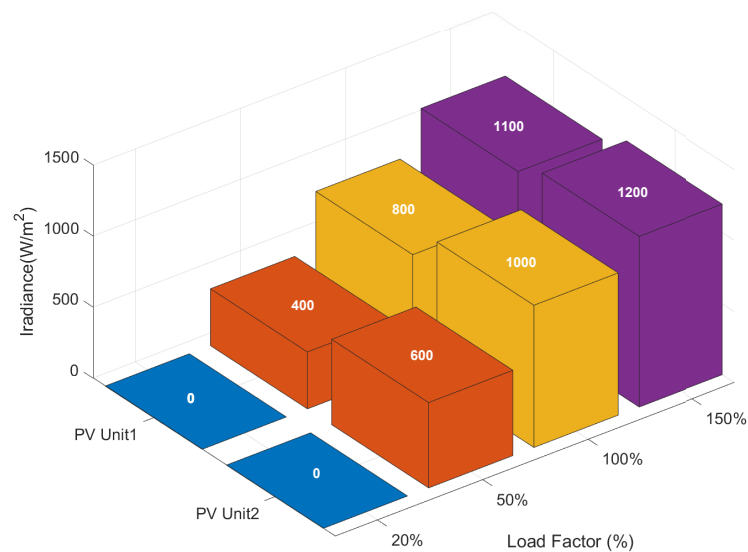


Figure 10. Variations in solar radiation corresponding to load fluctuations at each step.

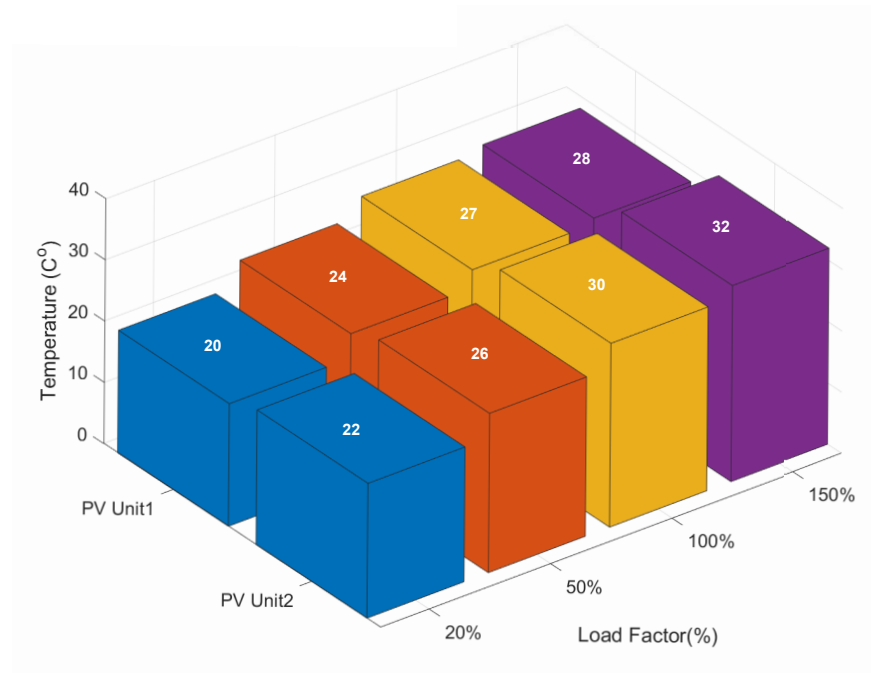


Figure 11. Temperature fluctuations corresponding to load changes at each step.

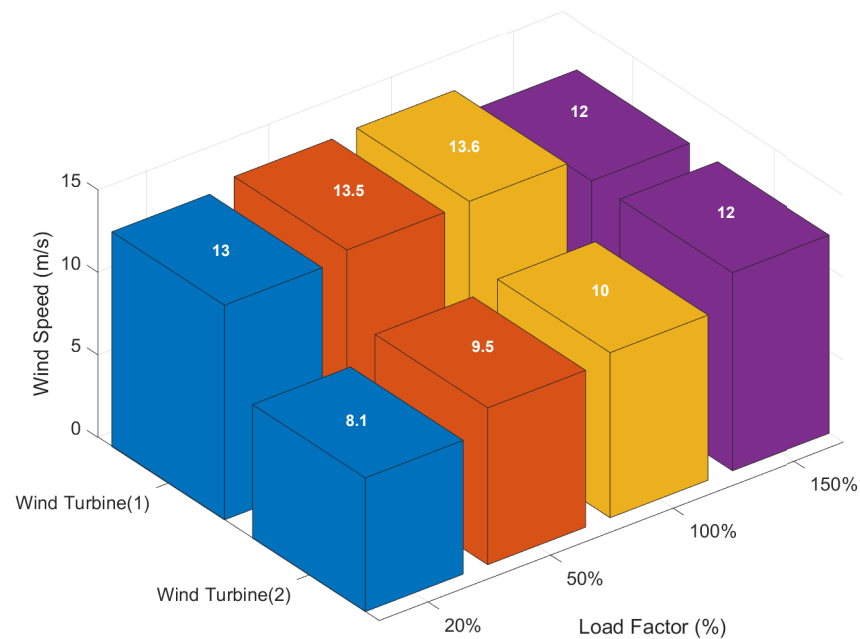


Figure 12. Alterations in wind speed corresponding to changes at each step.

5.2. Analytical Insights and Discussion (Unveiling the Findings)

In the initial phase, a thorough analysis was conducted to determine the most effective placement of BSSs and dynamic reconfiguration in the IEEE 118-, 69-, and 33-bus distribution networks and their interconnected subnetworks. This evaluation, utilizing the proposed methodology, considered both technical and economic considerations. Figures 13–15 illustrate the probability density functions of various desired objective functions throughout the optimization process.

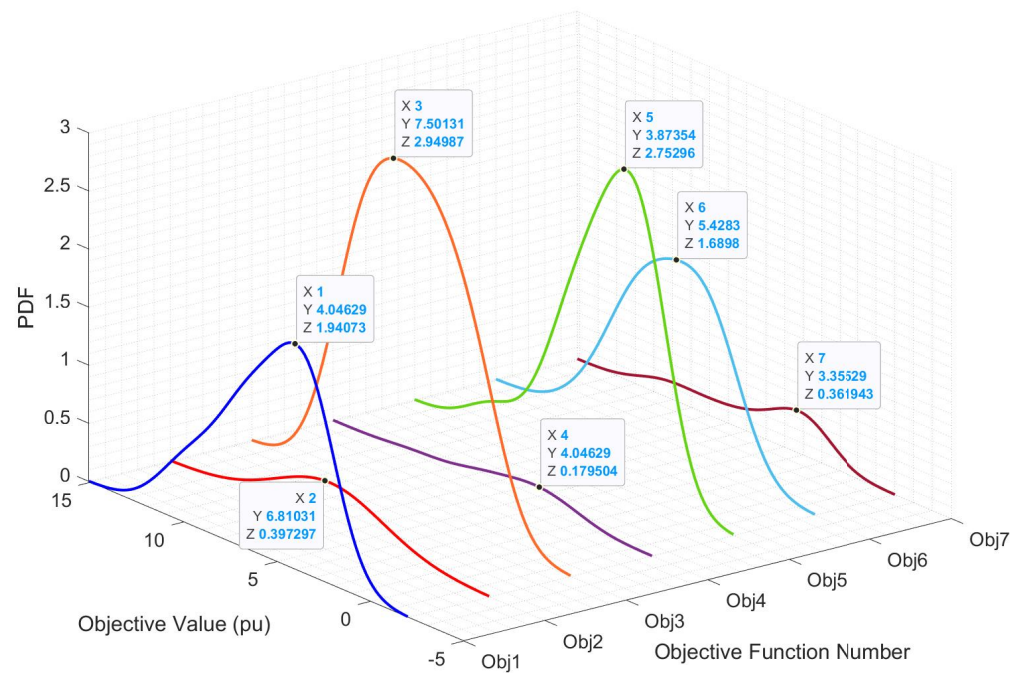


Figure 13. Probability density function of each objective function for IEEE 118-bus case study.

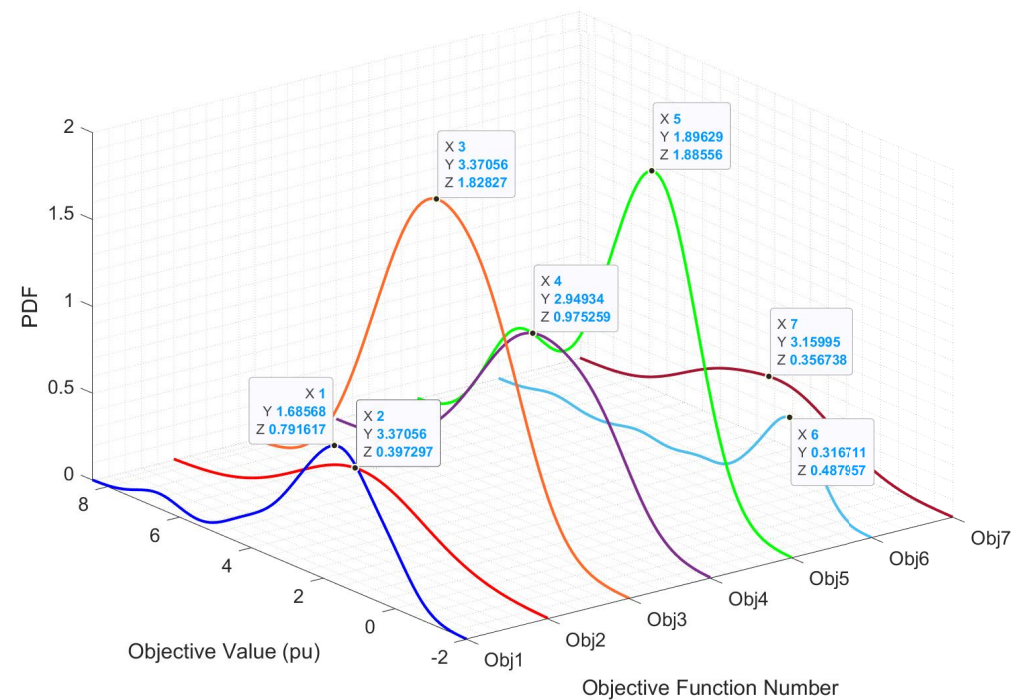


Figure 14. Probability density function of each objective function for IEEE 69-bus case study.

Subsequently, following the application of the proposed approach to identify the optimal positioning and operational states of BSSs, as well as the optimal states of dynamic switches in the IEEE 118-, 69-, and 33-bus systems across different load levels to enhance the economic and technical aspects of the system, a multiobjective optimization algorithm was employed. The resultant optimal solution can be summarized as follows. Figures 16 exhibits the optimal power generation profiles for each energy source during load fluctuations in the IEEE 118-, 69-, and 33-bus systems, respectively. Furthermore, Figures 17–19 portray the optimal placement and operational states of BSSs within the power networks of IEEE

118, 69, and 33 for each analyzed load percentage. These visuals offer valuable insights into the efficient management of power generation and storage within the network under varying load conditions.

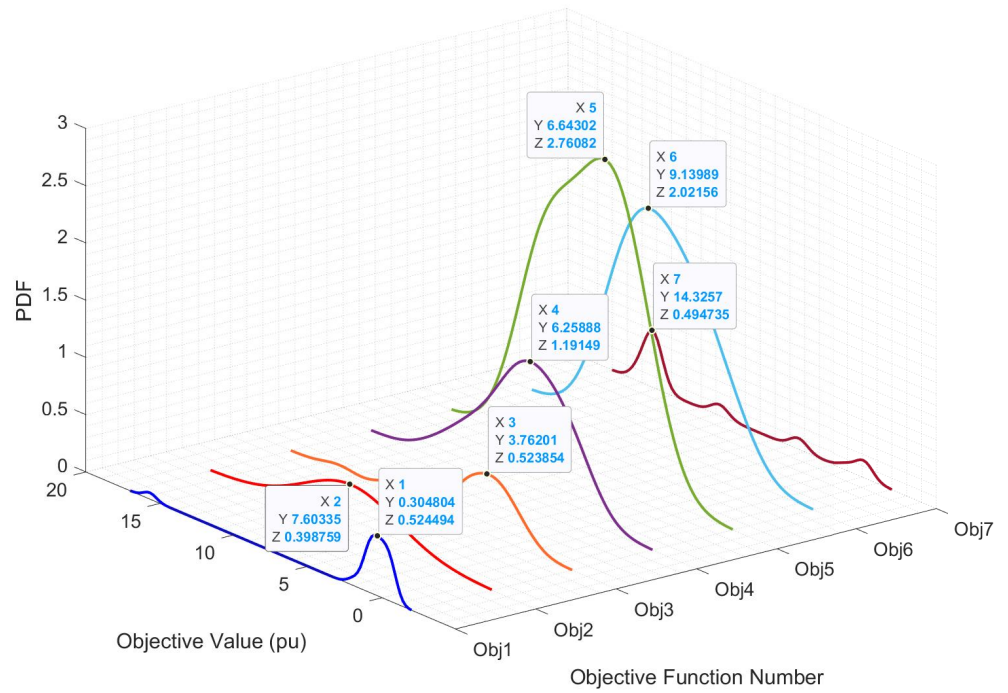


Figure 15. Probability density function of each objective function for IEEE 33-bus case study.

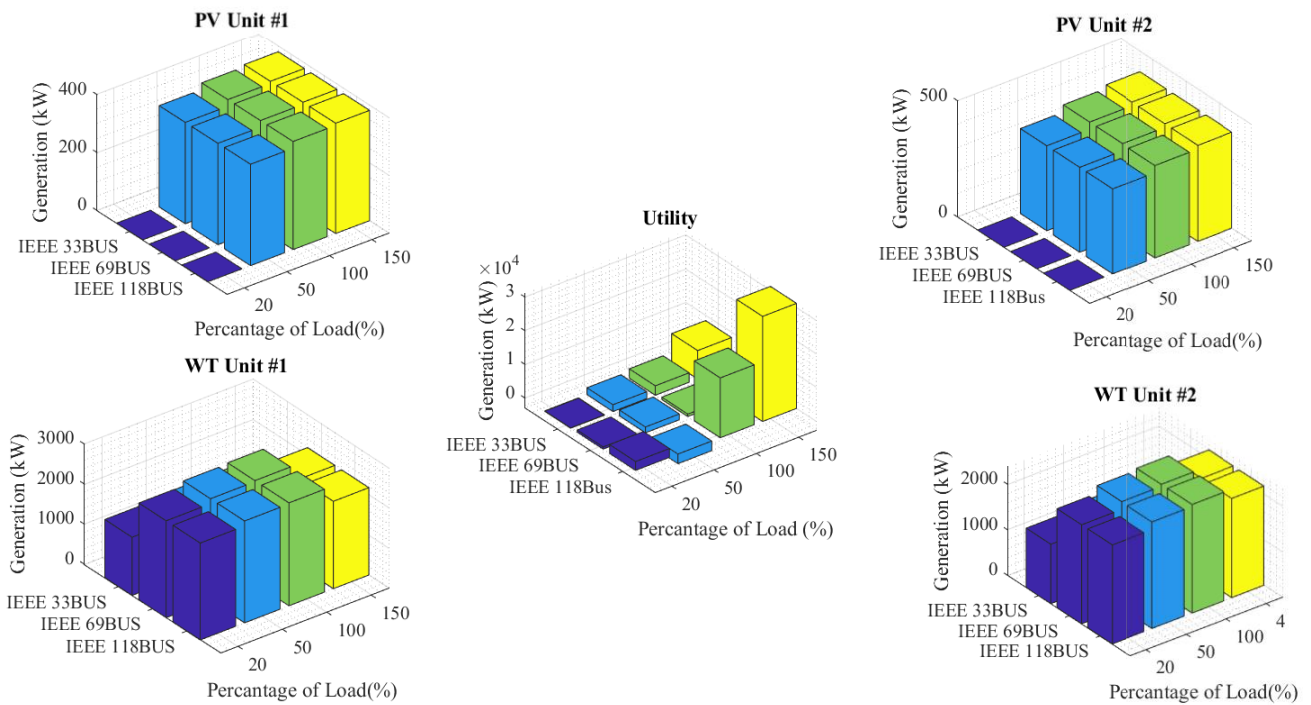


Figure 16. Optimal generation allocation for each unit at different load factors across various case studies (IEEE 118, 69, and 33 bus).

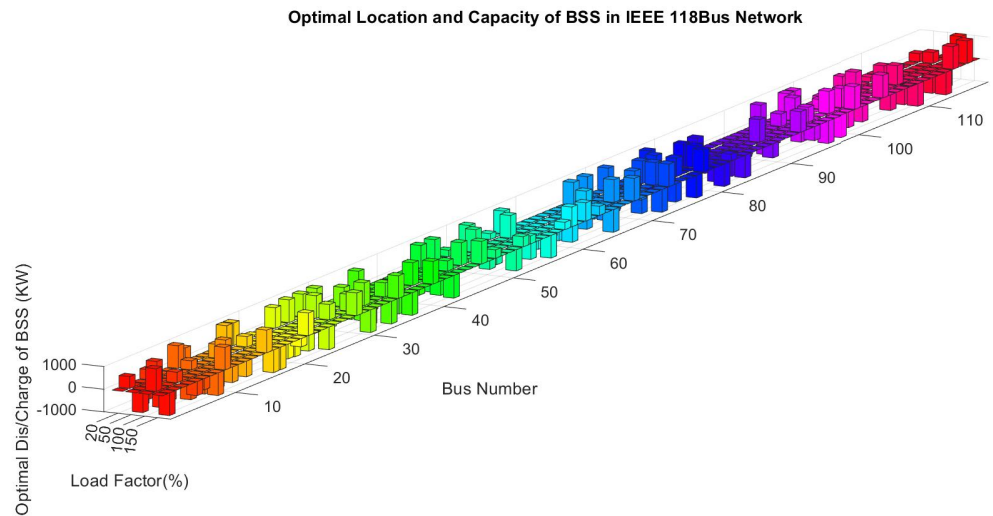


Figure 17. The optimal placement and optimal dis/charging of BSSs across various load percentages within the IEEE 118-bus network.

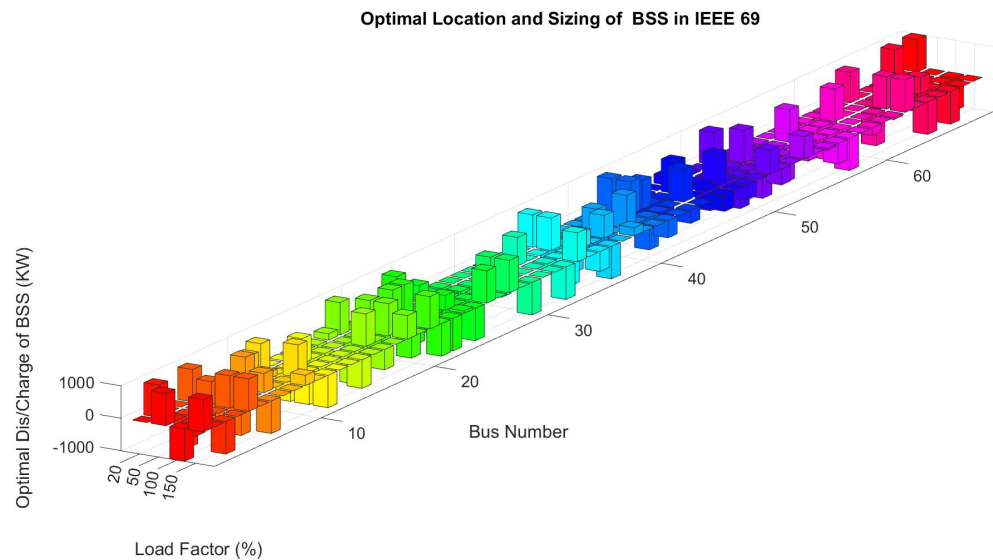


Figure 18. The optimal placement and optimal dis/charging of BSSs across various load percentages within the IEEE 69-bus network.

The precise findings detailing the optimal placement and operational configurations of BSSs for the IEEE 118-, 69-, and 33-bus systems are presented in Tables 2–4, correspondingly. These tables provide comprehensive information on the most effective locations and optimal charging/discharging states of BSSs within each network, offering valuable insights into the enhancement of power system performance and efficiency.

Moreover, the proposed framework delineates the ideal configurations of dynamic switches across varying load factors. Figures 20–22 illustrate the diverse states of interconnected switch breakers to ascertain the most efficient setup for the primary distribution network of IEEE 118, 69, and 33, respectively. This visualization aids in identifying the optimal configuration that maximizes the network's performance and efficiency.

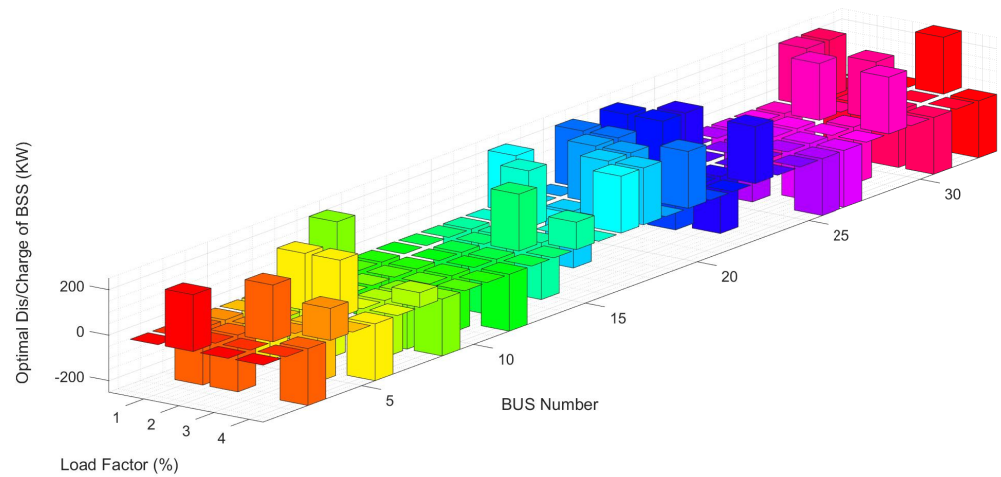


Figure 19. The optimal placement and optimal dis/charging of BSSs across various load percentages within the IEEE 33-bus network.

Table 2. Detailed outcomes outlining the optimal placement of BSSs within the IEEE 118-bus network for varying percentages of load.

Bus Number	Optimal State of Dis/Charging (kWh) of BSSs at Different Percentages of Nominal Load				Bus Number	Optimal State of Dis/Charging (kWh) of BSSs at Different Percentages of Nominal Load			
	20%	50%	100%	150%		20%	50%	100%	150%
1	0	0	0	0	60	−1000	0	0	874.548
2	523.571	−1000	1000	−1000	61	−519.82	0	0	0
3	0	−521.45	−846.81	0	62	0	−1000	−1000	807.008
4	−1000	1000	0	0	63	0	0	0	0
5	444.543	0	467.19	0	64	−1000	0	1000	399.456
6	0	−1000	0	−623.75	65	0	0	0	0
7	−1000	0	−1000	−501.03	66	1000	−1000	−47.964	−1000
8	0	0	0	0	67	0	0	0	0
9	1000	400.055	−1000	−1000	68	1000	0	1000	0
10	775.125	−1000	0	1000	69	−1000	−1000	0	1000
11	−1000	0	−1000	0	70	0	−770.4	0	−86.382
12	0	0	1000	0	71	1000	0	1000	0
13	0	612.979	−1000	0	72	−1000	−34.278	−1000	0
14	−1000	0	0	0	73	−567.78	0	0	−1000
15	0	0	−1000	0	74	0	1000	1000	1000
16	1000	0	0	1000	75	−1000	0	−232.3	−803.82
17	1000	454.839	−265.73	−1000	76	0	1000	0	0
18	0	−314.93	0	−1000	77	1000	−1000	818.687	0
19	0	0	−403.79	0	78	−1000	−1000	0	−1000
20	81.6294	0	0	0	79	0	0	−9.3727	1000
21	0	−970.19	−964.72	−372.11	80	0	1000	1000	0
22	0	0	−1000	1000	81	0	0	0	0
23	905.58	−1000	0	−23.363	82	−406.23	1000	0	−1000
24	0	0	−1000	0	83	0	0	−1000	301.726

Table 2. Cont.

Bus Number	Optimal State of Dis/Charging (kWh) of BSSs at Different Percentages of Nominal Load				Bus Number	Optimal State of Dis/Charging (kWh) of BSSs at Different Percentages of Nominal Load			
	20%	50%	100%	150%		20%	50%	100%	150%
25	1000	-768.75	0	-1000	84	0	0	0	0
26	0	0	0	0	85	-1000	-1000	-1000	-1000
27	1000	1000	676.006	0	86	2.12226	0	0	0
28	0	0	0	0	87	0	-1000	0	0
29	1000	0	0	1000	88	0	0	0	0
30	0	0	740.004	0	89	-1000	-778.33	1000	-625.07
31	-1000	854.918	0	-1000	90	0	0	0	0
32	0	0	1000	0	91	-1000	0	0	0
33	0	0	-1000	0	92	0	-1000	0	0
34	-1000	-1000	0	-1000	93	1000	0	-196.43	910.988
35	1000	0	620.332	1000	94	0	549.319	0	0
36	-1000	0	149.303	0	95	-1000	-478.27	-752.23	-620.77
37	-1000	0	-1000	-1000	96	0	1000	656.258	0
38	0	-1000	0	-237.66	97	1000	0	-96.738	-1000
39	0	-519.7	1000	0	98	1000	-1000	0	0
40	-1000	0	0	1000	99	-993.03	0	984.607	-1000
41	0	0	0	0	100	0	419.9	0	0
42	0	0	0	0	101	0	0	850.257	1000
43	0	0	-945.09	-1000	102	237.936	-1000	-1000	0
44	1000	-1000	452.465	0	103	0	0	0	0
45	-673.14	0	0	0	104	0	0	-1000	0
46	1000	-1000	1000	0	105	741.08	1000	0	1000
47	0	0	168.756	1000	106	405.013	0	0	0
48	284.628	0	0	0	107	0	0	0	0
49	0	0	-206.96	370.976	108	-827.6	0	-1000	0
50	0	1000	-96.276	0	109	207.884	777.042	851.119	33.8206
51	1000	0	0	0	110	210.632	0	-1000	-1000
52	0	-1000	0	-933.37	111	0	-450.68	0	0
53	-1000	-922.78	0	446.985	112	0	0	0	0
54	257.077	0	0	353.034	113	134.103	-1000	0	0
55	0	1000	0	0	114	0	0	-1000	-1000
56	1000	0	-1000	0	115	0	-234.4	0	1000
57	-521.32	-1000	0	-1000	116	362.797	477.75	-1000	0
58	-1000	0	0	0	117	0	0	0	1000
59	0	-1000	-416.79	326.779	118	0	-14.107	1000	0

Table 3. Detailed outcomes outlining the optimal placement of BSSs within the IEEE 69-bus network for varying percentages of load.

Bus Number	Optimal State of Dis/Charging (kWh) of BSSs at Different Percentages of Nominal Load				Bus Number	Optimal State of Dis/Charging (kWh) of BSSs at Different Percentages of Nominal Load			
	20%	50%	100%	150%		20%	50%	100%	150%
1	0	1000	−1000	1000	35	1000	1000	−1000	0
2	1000	0	−385.62	0	36	0	0	480.231	−614.18
3	0	−1000	0	−1000	37	−1000	−1000	0	−1000
4	0	0	0	0	38	0	0	701.071	0
5	1000	723.346	1000	1000	39	0	634.73	0	258.296
6	0	0	−1000	0	40	−1000	−1000	1000	0
7	−1000	0	0	−1000	41	−1000	0	0	0
8	0	1000	595.473	0	42	1000	1000	−1000	−531.26
9	0	0	0	0	43	0	876.503	0	0
10	621.568	196.493	0	319.34	44	0	0	0	−403.21
11	842.22	0	1000	0	45	−1000	−1000	1000	0
12	0	−1000	−1000	−1000	46	0	1000	0	−307.2
13	0	773.802	0	0	47	281.831	0	174.788	−508.75
14	0	0	−310.99	0	48	0	0	1000	0
15	0	−1000	0	−879.39	49	39.5753	−1000	0	−469.19
16	−1000	0	−1000	0	50	0	0	−1000	0
17	194.665	0	1000	−625.27	51	1000	−1000	0	743.649
18	1000	−1000	0	0	52	0	1000	−1000	−489.12
19	0	1000	1000	727.966	53	−1000	−111.68	0	0
20	0	−991.96	0	0	54	0	0	−824.4	682.179
21	−1000	1000	−1000	995.552	55	−1000	−1000	0	0
22	0	1000	−221.91	−1000	56	0	1000	−486.82	−57.385
23	1000	−1000	0	−1000	57	0	0	0	−640.08
24	0	0	456.635	76.5487	58	0	0	0	−1000
25	407.979	−1000	−697.48	−1000	59	−1000	−1000	−1000	0
26	0	−369.67	−1000	1000	60	0	1000	0	−236.62
27	−874.55	−1000	0	0	61	−1000	0	0	0
28	0	−1000	1000	1000	62	0	0	−968.4	−65.005
29	0	0	−391.5	0	63	943.29	0	1000	1000
30	0	0	0	−1000	64	0	−246.06	0	0
31	0	0	0	0	65	0	−272.54	0	−1000
32	−536.92	878.989	0	0	66	−209.87	0	501.54	0
33	0	0	−212.52	−1000	67	1000	0	−611.79	−1000
34	0	0	0	897.894	68	0	−1000	0	0
					69	1000	0	−1000	0

Table 4. Detailed outcomes outlining the optimal placement of BSSs within the IEEE 33-bus network for varying percentages of load.

Bus Number	Optimal State of Dis/Charging (kWh) of BSSs at Different Percentages of Nominal Load				Bus Number	Optimal State of Dis/Charging (kWh) of BSSs at Different Percentages of Nominal Load			
	20%	50%	100%	150%		20%	50%	100%	150%
1	0	250	0	0	17	250	0	0	250
2	0	0	0	0	18	0	-250	250	250
3	-250	-250	250	-250	19	0	250	250	0
4	-250	0	0	140.857	20	250	250	0	250
5	0	0	-250	0	21	0	0	-161.55	0
6	-250	250	250	-250	22	250	250	0	0
7	0	-250	0	0	23	-250	250	-250	250
8	-250	0	-250	64.5045	24	0	0	0	0
9	250	0	-250	-250	25	0	0	0	0
10	0	0	0	0	26	0	-250	0	-250
11	-250	-250	-250	0	27	-96.052	0	-250	-250
12	0	0	0	-250	28	0	-76.418	0	0
13	0	-250	-250	0	29	-250	250	-250	250
14	0	0	250	0	30	250	0	250	0
15	-250	-250	-250	120.263	31	250	0	-250	-250
16	0	250	0	0	32	-250	0	0	0
					33	0	0	250	-250

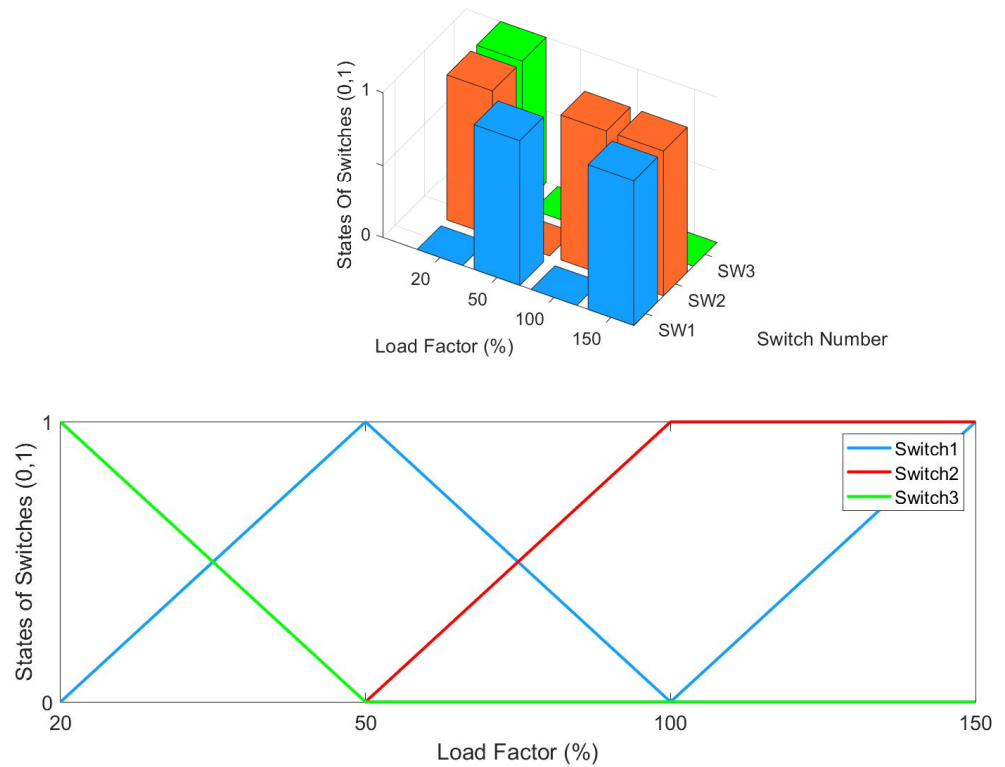


Figure 20. Optimal state of dynamic coupled switches in IEEE 118-bus network within different load factors.

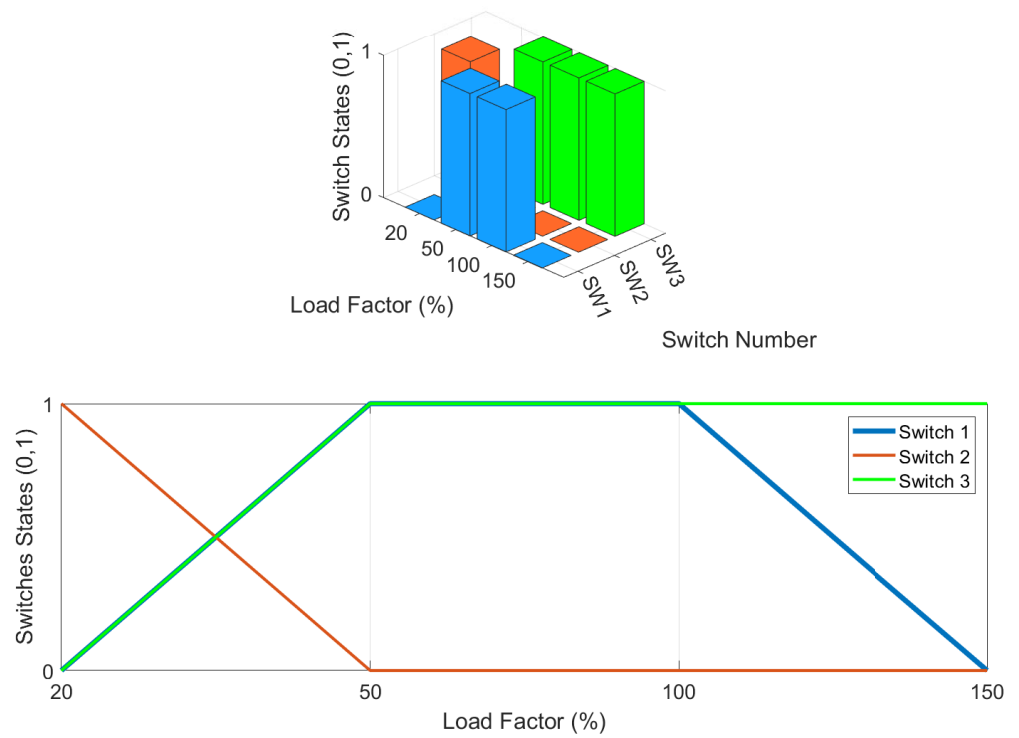


Figure 21. Optimal state of dynamic coupled switches in IEEE 69-bus network within different load factors.

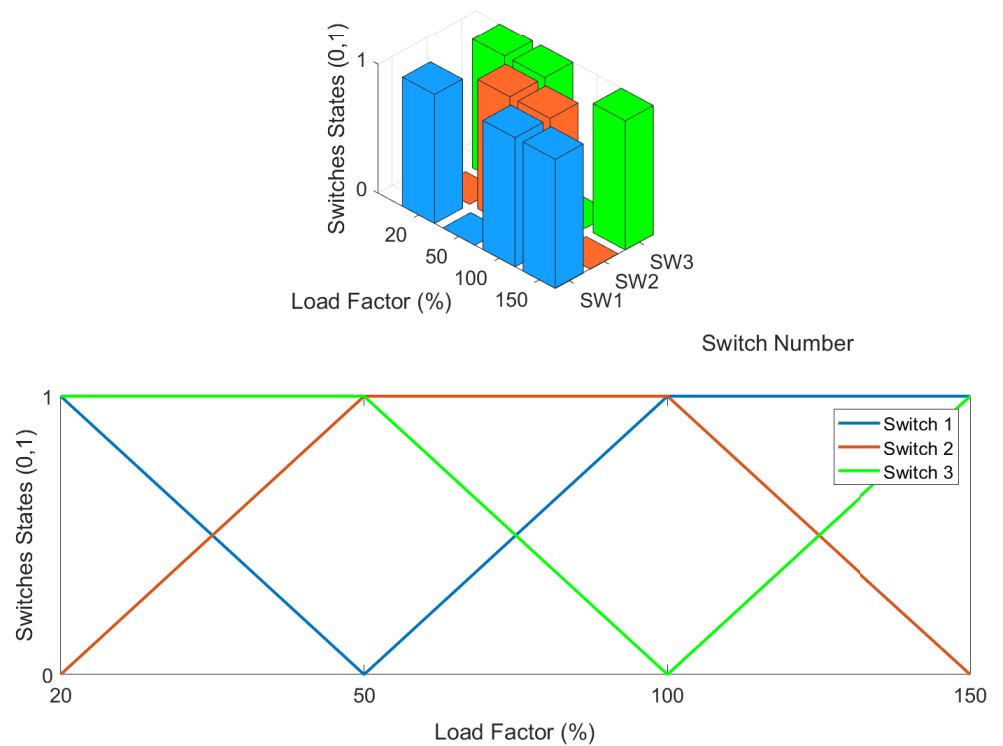


Figure 22. Optimal state of dynamic coupled switches in IEEE 33-bus network within different load factors.

Furthermore, Tables 5–7 were meticulously compiled to showcase a comprehensive analysis of the proposed methodology’s performance compared to existing approaches. The comparison covers various key metrics such as economic viability, power quality improvements, reliability enhancements, and network security considerations. These tables offer a detailed evaluation of the optimal BSS placement program’s effectiveness over the study period within the IEEE 118-, 69-, and 33-bus networks, providing valuable insights into the overall impact and benefits of the proposed method.

Table 5. Comparison between the proposed method and other state-of-the-art approaches in the context of the IEEE 118-bus network.

Method	Operating Cost (\$)	Losses (kW)	Voltage Deviation (pu)	(EENS) (kWh)	VSI (pu)	Sum of Short-Circuit-Level Changes (pu)
Proposed method	12,687.72 ✓	1.33 ✓	1.36 ✓	62.62 ✓	9.982 ✓	1.93 ✓
[2,3]	18,452.63 ✓	6.62 ✓	6.791 ✗	114.21 ✗	5.32 ✓	4.25 ✗
[7,10]	24,384.21 ✓	8.274 ✓	5.217 ✗	87.64 ✓	4.28 ✗	6.54 ✗
[14,19]	21,628.64 ✓	11.427 ✗	1.87 ✓	314.21 ✗	7.81 ✗	12.37 ✗

Table 6. Comparison between the proposed method and other state-of-the-art approaches in the context of the IEEE 69-bus network.

Method	Operating Cost (\$)	Losses (kW)	Voltage Deviation (pu)	(EENS) (kWh)	VSI (pu)	Sum of Short-Circuit-Level Changes (pu)
Proposed method	1153.01 ✓	15.09 ✓	0.81 ✓	31.19 ✓	5.00 ✓	0.751 ✓
[2,3]	1453.21 ✓	21.12 ✓	2.35 ✗	68.21 ✗	4.21 ✓	8.51 ✗
[7,10]	1712.31 ✓	16.32 ✓	6.31 ✗	38.54 ✓	1.24 ✗	10.24 ✗
[14,19]	1471.14 ✓	18.25 ✗	3.98 ✓	48.56 ✗	2.94 ✗	11.71 ✗

Table 7. Comparison between the proposed method and other state-of-the-art approaches in the context of the IEEE 33-bus network.

Method	Operating Cost (\$)	Losses (kW)	Voltage Deviation (pu)	(EENS) (kWh)	VSI (pu)	Sum of Short-Circuit-Level Changes (pu)
Proposed method	3401.21 ✓	1.82 ✓	0.29 ✓	56.08 ✓	1.55 ✓	0.929 ✓
[2,3]	5061.28 ✓	3.21 ✓	2.63 ✗	63.21 ✗	1.23 ✓	1.24 ✗
[7,10]	4716.25 ✓	4.612 ✓	3.83 ✗	59.32 ✓	0.68 ✗	5.28 ✗
[14,19]	4781.21 ✓	8.241 ✗	0.81 ✓	71.23 ✗	0.94 ✗	3.67 ✗

The analysis of the simulation results from the IEEE 33-, 69-, and 118-bus test systems, detailed in Tables 5–7, underscores the superiority of the proposed method over existing approaches in both economic and technical network metrics. This achievement is particularly remarkable given the historical oversight of reliability and power quality indicators in prior studies. The innovative methodology effectively optimizes distributed generation control within the distribution network and intelligent microgrids, notably by strategically managing the operation, such as the charging and discharging of BSSs at key locations and dynamically switching energy paths in power line transmission. For example, the evaluation presented in Tables 5–7 reveals that the energy storage systems in the IEEE 118-, 69-, and 33-bus networks were charged during periods of low demand, typically ranging from 20% to 150% of nominal load. This strategic charging aligns technical aspects like

reliability and power quality with economic considerations such as operational efficiency and generation costs.

6. Conclusions

In the contemporary landscape, intelligent distribution microgrids represent a fusion of autonomous units that act as energy consumers and generators, pivotal for optimizing economic efficiency and ensuring the secure functioning of smart distribution networks. The dynamic operation of charging and discharging BSSs within these networks can elevate these units to intelligent network nodes, especially when dynamic switches alter energy pathways during network reconfiguration. This capability enables the effective management of a substantial portion of locally generated energy, catering to both generators and consumers. This study introduces a novel approach for the strategic placement of BSSs in conjunction with dynamic network reconfiguration, considering technical power system aspects such as power quality and reliability alongside economic factors. By orchestrating the generation resources and harnessing the charging and discharging capabilities of BSSs within the distribution network, this solution aims to optimize energy transfer pathways while mitigating potential risks associated with purely economic exploitation. The formulation of an objective function in a comprehensive BSS placement program for the network necessitates the inclusion of not only economic metrics but also reliability and security indicators like EENS and stability in short-circuit connection levels. By integrating these diverse factors into a multiobjective optimization algorithm for simultaneous BSS placement and dynamic network reconfiguration, the framework ensures effective management of anticipated energy shortages and protection setting disruptions during the economic operation of distribution networks and interconnected microgrids, particularly under peak load conditions. Leveraging the charge and discharge capabilities of microgrid networks in tandem with optimal energy management facilitates the achievement of these objectives. Comparative analysis between the proposed method and prior approaches demonstrates consistent and substantial enhancements in technical and economic indicators, emphasizing the significance of incorporating reliability and security considerations into the formulation of BSS placement strategies. It should be noted that the accuracy of the proposed optimal planning method for BSSs could be influenced by uncertainties in factors such as future energy demand, technological advancements, and regulatory changes. Additionally, the effectiveness of the integrated approach in addressing grid stability and reliability may vary depending on specific grid characteristics and local conditions. On the other hand, future research could focus on refining the optimization model by incorporating more detailed and accurate data, such as real-time grid measurements and user behavior patterns.

Author Contributions: W.K.M.A.-Z.: conceptualization, methodology, experimentation, validation, formal analysis, investigation, data curation, writing—original draft, writing—review and editing, and visualization. A.I.: conceptualization, methodology, validation, investigation, resources, writing—original draft, writing—review and editing, visualization, supervision, and project administration. All authors have read and agreed to the published version of the manuscript.

Funding: This research received no external funding.

Institutional Review Board Statement: Not applicable.

Informed Consent Statement: Not applicable.

Data Availability Statement: All data available in the article.

Acknowledgments: The author (WALEED KHALID MAHMOOD AL-ZAIDI) would like to acknowledge that this paper is submitted in partial fulfillment of the requirements for the PhD degree at Yildiz Technical University.

Conflicts of Interest: The authors declare no conflicts of interest.

Abbreviations

The following abbreviations are used in this manuscript:

DG	Distributed generation
BSS	Battery swapping station
DER	Distributed energy resources
EV	Electric vehicle
EBs	Electric buses
VSC	Voltage source converter
GWO	Gray wolf optimization
PSO	Particle swarm optimization
EMS	Energy management systems
RDS	Radial distribution system
EENS	Expected energy not served
RE	Renewable energy
TR	Traditional energy
VSI	Voltage sensitivity index
PLSF	Power loss sensitivity factor
ESS	Energy storage systems
MT	Microturbine

List of Nomenclature

P_{EV_0}	The initial charging power of the electric vehicle.
$P_{EV_{max}}$	The maximum charging power of the electric vehicle.
α	The charging battery time constant of the electric vehicle.
t_{max}	Signifies the total time needed to charge the electric vehicle's battery from zero charge to maximum charge.
P_N	The probability coefficient of power consumption in an electric vehicle charging station.
λ	The success rate of a vehicle in accessing the charging converter.
μ	The success rate of a vehicle in completing its battery charging.
$\rho = \lambda/\mu.c$	Stands for the number of charging stations for electric vehicles.
C	The number of BSSs for electric vehicles.
P_{PV}	PV system output power at the maximum power point.
P_{wt}	Wind turbine output power.
$P_{(PV,STC)}$	Nominal PV power at the maximum power point and standard conditions.
G_T	Radiation amount in standard conditions.
γ	Temperature coefficient.
T_j	The temperature of the solar cells.
N_{PV_s}	The number of series modules.
N_{PV_p}	The number of parallel modules.
V_{ci}	Lower cutoff speed.
V_r	Nominal speed of the wind turbine.
V_{co}	Upper cutoff speed.
P_R	Nominal power of the wind turbine.
$C_{DG,t}^{OP}$	The cost of operating in each time interval t .
$C_{DG,t}^{EM}$	The cost associated with the pollution of the units in each time interval t .
$\lambda_{(CO_2)}$	Penalty factor for CO ₂ production.
$\lambda_{(SO_2)}$	Penalty factor for SO ₂ production.
$\lambda_{(NO_x)}$	Penalty factor for NO _x production.
$P_{BSS}(t)$	The powers of the BSS.
$P_{DG}(t)$	The powers of DG.
$P_g(t)$	The powers of the grid.
$P_{ch}(t)$	Charging powers of BSS.
$P_{dch}(t)$	Discharging powers of BSS.

$SOC(t)$	State of charge.
$E_{ch}(t)$	Charging energy.
$E_{dch}(t)$	Discharging energy.
σ	Denotes the number of equality constraints.
η_{ch}	Charging/discharging efficiency.
η_{Conv}	Converter efficiency.
$C_{rep,batt}$	The storage replacement cost.
η_{rt}	The roundtrip efficiency of the storage.
$C_{BSS}^{constant}$	The constant cost of the battery swapping station (BSS).
$NOCT$	Normal operating cell temperature of the PV system.
P_R	The output power of these renewable units.
ζ_R	The variable cost associated with renewable generation units.
ψ_R^{cte}	The constant costs related to the renewable units.
V_k & V_k^*	The Voltage of each bus in the network before and after any changes in the network.
$R_{eq,i}$	Resistance of the line.
$X_{eq,i}$	Reactance of the line.
$P_{Lm,i}$	The aggregate active power of all nodes.
$Q_{Lm,i}$	The aggregate reactive power of all nodes.
S_i	Dynamic switch.
γ_k	The weight coefficient associated with the objective functions.

References

- Kocer, M.C.; Onen, A.; Jung, J.; Gultekin, H.; Albayrak, S. Optimal location and sizing of electric bus battery swapping station in microgrid systems by considering revenue maximization. *IEEE Access* **2023**, *11*, 41084–41095. [\[CrossRef\]](#)
- Zeng, B.; Luo, Y.; Liu, Y. Quantifying the contribution of EV battery swapping stations to the economic and reliability performance of future distribution system. *Int. J. Electr. Power Energy Syst.* **2022**, *136*, 107675. [\[CrossRef\]](#)
- Guo, Y.; Lei, X.; Wang, Q. Capacity coordination planning of isolated microgrid and battery swapping station based on the quantum behavior particle swarm optimization algorithm. *Int. Trans. Electr. Energy Syst.* **2021**, *31*, e12804. [\[CrossRef\]](#)
- Zhang, N.; Zhang, Y.; Ran, L.; Liu, P.; Guo, Y. Robust location and sizing of electric vehicle battery swapping stations considering users' choice behaviors. *J. Energy Storage* **2022**, *55*, 05561. [\[CrossRef\]](#)
- Boonraksa, T.; Boonraksa, P.; Pinthurat, W.; Marungsri, B. Optimal Battery Charging Schedule for a Battery Swapping Station of an Electric Bus with a PV Integration Considering Energy Costs and Peak-to-Average Ratio. *IEEE Access* **2021**, *11*, 36280–36295. [\[CrossRef\]](#)
- Nematollahi, A.F.; Shahinzadeh, H.; Nafisi, H.; Vahidi, B.; Amirat, Y.; Benbouzid, M. Sizing and siting of DERs in active distribution networks incorporating load prevailing uncertainties using probabilistic approaches. *Appl. Sci.* **2008**, *10*, 142–149. [\[CrossRef\]](#)
- Sui, Q.; Li, F.; Wu, C.; Feng, Z.; Lin, X.; Wei, F.; Li, Z. Optimal scheduling of battery charging–swapping systems for distribution network resilience enhancement. *Energy Rep.* **2022**, *8*, 6161–6170. [\[CrossRef\]](#)
- Zhang, M.; Li, W.; Yu, S.S.; Wen, K.; Zhou, C.; Shi, P. A unified configurational optimization framework for battery swapping and charging stations considering electric vehicle uncertainty. *Energy* **2021**, *218*, 119536. [\[CrossRef\]](#)
- Wang, Z.; Hou, S.; Guo, W. Inventory management of battery swapping and charging stations considering uncertainty. *Int. J. Electr. Power Energy Syst.* **2024**, *155*, 109528. [\[CrossRef\]](#)
- Fokui, W.S.T.; Saulo, M.J.; Ngoo, L. Optimal placement of electric vehicle charging stations in a distribution network with randomly distributed rooftop photovoltaic systems. *IEEE Access* **2021**, *9*, 132397–132411. [\[CrossRef\]](#)
- Yuan, Z.; Wang, W.; Wang, H.; Yildizbasi, A. A new methodology for optimal location and sizing of battery energy storage system in distribution networks for loss reduction. *J. Energy Storage* **2020**, *29*, 101368. [\[CrossRef\]](#)
- Jordehi, A.R.; Javadi, M.S.; Catalão, J.P. Optimal placement of battery swap stations in microgrids with micro pumped hydro storage systems, photovoltaic, wind and geothermal distributed generators. *Int. J. Electr. Power Energy Syst.* **2021**, *125*, 106483. [\[CrossRef\]](#)
- Wang, H.; Ma, H.; Liu, C.; Wang, W. Optimal scheduling of electric vehicles charging in battery swapping station considering wind-photovoltaic accommodation. *Electr. Power Syst. Res.* **2021**, *199*, 107451. [\[CrossRef\]](#)
- Koirala, K.; Tamang, M. Planning and establishment of battery swapping station-A support for faster electric vehicle adoption. *J. Energy Storage* **2022**, *51*, 104351. [\[CrossRef\]](#)
- Boonraksa, T.; Boonraksa, P.; Marungsri, B.; Sarapan, W. Optimal PV Sizing of the PV-Based Battery Swapping Stations on the Radial Distribution System using Whale Optimization Algorithm. In Proceedings of the 2022 International Conference on Power, Energy and Innovations (ICPEI), Pattaya Chonburi, Thailand, 19–21 October 2022; pp. 1–4.
- Shaker, M.H.; Farzin, H.; Mashhour, E. Joint planning of electric vehicle battery swapping stations and distribution grid with centralized charging. *J. Energy Storage* **2023**, *58*, 106455. [\[CrossRef\]](#)

17. Garcia-Guarin, J.; Infante, W.; Ma, J.; Alvarez, D.; Rivera, S. Optimal scheduling of smart microgrids considering electric vehicle battery swapping stations. *Int. J. Electr. Comput. Eng.* **2020**, *10*, 5093.
18. Ko, H.; Pack, S.; Leung, V.C. An optimal battery charging algorithm in electric vehicle-assisted battery swapping environments. *IEEE Trans. Intell. Transp. Syst.* **2020**, *23*, 3985–3994. [[CrossRef](#)]
19. Balu, K.; Mukherjee, V. Optimal allocation of electric vehicle charging stations and renewable distributed generation with battery energy storage in radial distribution system considering time sequence characteristics of generation and load demand. *J. Energy Storage* **2023**, *59*, 106533. [[CrossRef](#)]
20. Qiao, X.; Luo, Y.; Xiao, J.; Li, Y.; Jiang, L.; Shao, X.; Xu, J.; Tan, Y.; Cao, Y. Optimal scheduling of distribution network incorporating topology reconfiguration, battery energy system and load response. *CSEE J. Power Energy Syst.* **2020**, *8*, 743–756.
21. Sultana, U.; Khairuddin, A.B.; Sultana, B.; Rasheed, N.; Qazi, S.H.; Malik, N.R. Placement and sizing of multiple distributed generation and battery swapping stations using grasshopper optimizer algorithm. *Energy* **2018**, *165*, 408–421. [[CrossRef](#)]
22. He, C.; Zhu, J.; Li, S.; Chen, Z.; Wu, W. Sizing and locating planning of EV centralized-battery-charging-station considering battery logistics system. *IEEE Trans. Ind. Appl.* **2022**, *58*, 5184–5197. [[CrossRef](#)]
23. Erdinç, O. Considering the combinatorial effects of on-site distributed generation and battery-to-X option availability in electric vehicle battery swap station operation. *Sustain. Energy Grids Netw.* **2021**, *26*, 100472. [[CrossRef](#)]
24. Jimenez, A.; Garcia, N. Power flow modeling and analysis of voltage source converter-based plug-in electric vehicles. In Proceedings of the IEEE Power and Energy Society General Meeting, Detroit, MI, USA, 24–28 July 2011; pp. 1–6.
25. Yudai, H.; Osamu, K. A safety stock problem in battery switch stations for electric vehicles. In Proceedings of the Eighth International Symposium on Operations Research and Its Applications (ISORA), Zhangjiajie, China, 20–22 September 2009; pp. 332–339.
26. Al-Zaidi, W.K.M.; Inan, A. Optimal Placement of Battery Swapping Stations for Power Quality Improvement: A Novel Multi Techno-Economic Objective Function Approach. *Energies* **2023**, *17*, 110. [[CrossRef](#)]
27. Qawaqzeh, M.; Al_Issa, H.A.; Buinyi, R.; Bezruchko, V.; Dikhtyaruk, I.; Miroshnyk, O.; Nitsenko, V. The assess reduction of the expected energy not-supplied to consumers in medium voltage distribution systems after installing a sectionalizer in optimal place. *Sustain. Energy Grids Netw.* **2023**, *34*, 101035. [[CrossRef](#)]
28. Dereli, S. A new modified grey wolf optimization algorithm proposal for a fundamental engineering problem in robotics. *Neural Comput. Appl.* **2021**, *33*, 14119–14131.

Disclaimer/Publisher’s Note: The statements, opinions and data contained in all publications are solely those of the individual author(s) and contributor(s) and not of MDPI and/or the editor(s). MDPI and/or the editor(s) disclaim responsibility for any injury to people or property resulting from any ideas, methods, instructions or products referred to in the content.